Thus, insertion predominates for most alkene substrates, whereas σ-bond metathesis is competitive with insertion for several alkynes studied here.

The mechanistic interpretation of the reactions of **1** is simplified because of the absence of accessible higher zirconium oxidation states. Thus, oxidative addition and reductive elimination, often invoked to explain the reactions of bare metal ions,[29,46] are highly improbable mechanistic sequences in the reactions of **1**. This suggests that mechanisms other than oxidative addition/reductive elimination may also be applied to the analogous reactions of bare metal ions in the gas phase.

We have demonstrated that processes observed in the solution reactions of d^0f^n organometallic complexes are evidently observed for the $Cp_2ZrCH_3^+$ in the gas phase. The gas-phase investigation of cation **1** provides a unique opportunity to characterize the σ-bond metathesis and insertion reaction sequences in the absence of solvent, especially because the results can be compared to the same processes for analogous complexes in solution. The present results also suggest that information pertaining to the possible synthesis of a variety of new organometallic complexes and possible side reactions may be obtained through these types of gas-phase studies.

Experimental Section

Results for ion/molecule reactions were obtained by using Fourier transform ion cyclotron resonance mass spectrometry. Two different mass spectrometers were employed for reaction studies. Data used in determination of rate coefficients were acquired with a Nicolet FTMS 1000 (3.0 T). Product distributions were determined mainly on the second system, which is constructed around a 2.0-T magnet. The second system is very similar to the FTMS 1000; the main difference is a larger vacuum chamber and increased pumping capability. A check of product distributions for the same reactions determined in the two systems shows good agreement within experimental error.

Electron impact (EI) (11-12 eV) on $Cp_2Zr(CH_3)_2$ ($p \approx 10^{-8}$-10^{-7} Torr) yields predominantly $Cp_2ZrCH_3^+$ and Cp_2Zr^+. Cp_2Zr^+ and any ionized substrate are ejected from the ICR cell isolating $Cp_2ZrCH_3^+$ for reaction studies. Substrates are generally present at pressures ca. 10^{-7}-10^{-6} Torr. Argon or krypton are used as buffer gases at pressures in the 10^{-6}-10^{-5} Torr range. A thermalization time precedes the acquisition of data and permits $Cp_2ZrCH_3^+$ multiple collisions with buffer gas to ensure reactions are studied under thermal conditions.

The formation of binuclear zirconium ions $Cp_4Zr_2(CH_3)_n^+$ (n = 0-2) limits the study of ion/molecule reactions to those with rate coefficients above $\sim 10^9$ M^{-1} s^{-1} (10^{-12} cm^3 s^{-1}). However, reactions with slightly smaller rate coefficients may be investigated if pressures of $Cp_2Zr(CH_3)_2$ are reduced to the low 10^{-8} Torr range.

Water reacts with **1** rapidly, even when present as a slight impurity in a substrate (eq 38). Therefore, drying of substrates is imperative.

$$Cp_2ZrCH_3^+ + H_2O \rightarrow Cp_2ZrOH^+ + CH_4 \quad (38)$$

The method used for determination of rate coefficients was described previously[7a] and yields values estimated to be within ±30% of the absolute rate constants. Product distributions and rate constants are reported in the text with 95% confidence limits.

$Cp_2Zr(CH_3)_2$ and $Cp_2Zr(CD_3)_2$ were synthesized according to a literature preparation[55] and analyzed by NMR and mass spectrometry. Deuteromethyllithium was synthesized in dry diethyl ether from CD_3I purchased from Aldrich. Mass spectrometric analysis of $Cp_2Zr(CD_3)_2$ indicated >99% deuteration.

Collision-induced dissociation experiments are performed by imparting kinetic energy to a given ion (by radio frequency excitation) in the presence of an inert gas at pressures in the range 5×10^{-6} to 1×10^{-5} Torr. Upon collision with the neutral, the fragmentation of the parent ion to produce a daughter ion spectrum may be used to provide structural information about the parent ion. The kinetic energy of the parent ion prior to collision can be controlled by varying the radio frequency power applied, and the dependence of the endothermic fragmentation pathways on ion translational energy can be probed.

Double-resonance experiments provide means for determining the origin of a product ion (i.e., identifies the ion from which a product ion arises following an ion/molecule reaction). By use of the ion ejection capabilities of the FTICR, various ions in a complex mass spectrum can be removed from the trap to isolate a single type of ion. The reactions of this ion with added neutrals can then be followed independently. Alternatively, in a more traditional double-resonance experiment, a suspected precursor ion is continuously ejected from the trap during the reaction time. A reduced yield of a given product ion indicates the contribution of the ejected ion to the observed product ion mass spectrum.

Liquid substrates were purchased from Aldrich in high purity and used after drying over CaH_2. C_2D_4 and D_2 were purchased from Cambridge Isotope Labs and used as received. All other gases were purchased from commercial sources in high purity and used without further purification.

Acknowledgment. Support for this work was provided by a grant from the National Science Foundation (CHE-8700765), which is gratefully acknowledged. We also thank R. F. Jordan and J. I. Brauman for helpful discussions and the reviewers for insightful suggestions.

Selectivity as a Function of Anionic Base Properties in the Gas-Phase Reactions of Dimethyl Sulfite

Joseph J. Grabowski* and Rachel C. Lum

Contribution from the Department of Chemistry, Harvard University, 12 Oxford Street, Cambridge, Massachusetts 02138. *Received April 26, 1989*

Abstract: The thermally equilibrated gas-phase reactions of dimethyl sulfite ($CH_3OSO_2CH_3$), in a helium bath gas at 300 K, with a variety of anions ranging from amide, phenide, and allyl anions to nitromethide and hydrosulfide, have been quantitatively examined using the flowing afterglow technique. A master reaction scheme, composed of four competitive reaction pathways, is presented to account for the experimental observations. Of primary importance in selectivity is the structure of the anionic nucleophile and then its basicity. Strongly basic, localized, heteroatomic nucleophiles yield larger amounts of elimination products compared to localized carbon bases of comparable basicity. While most anions yield methyl substitution products, localized bases are much more nucleophilic at carbon than delocalized carbon bases. For nucleophilic attack at sulfur the opposite trend is found, delocalized carbon bases being most nucleophilic at this site. Only the weakly basic cyclopentadienide and nitromethide anions were found to react with dimethyl sulfite solely by termolecular adduct formation. Anomalies in the observations for acetaldehyde enolate, cyanomethide, and anilide anions are suggestive of reaction via the heteroatomic sites of these nucleophiles. The new level of chemical understanding developed from the overall reaction scheme defined will help design future gas-phase experiments to probe specific reaction mechanisms.

The chemistry of organic sulfites is well over 100 years old; this functionality has been the subject of numerous studies. Organic sulfites have intriguing reactivity and structural features in addition to practical applications as insecticides and plant growth regulators

0002-7863/90/1512-607$02.50/0

among others.[1] On initial inspection, the organic chemistry of sulfites can be anticipated to behave analogously to that of esters. For example, Bristow and Tillet[2] have shown that in the liquid phase dialkyl sulfites undergo rapid alkoxy exchange catalyzed by either acid or base and that nucleophilic attack (by alkoxide ions) at carbon is much slower; results that are in accord with our understanding of transesterification of esters by alcohols.

Recent gas-phase experimental and theoretical studies on the reactions of alkoxides with esters has dramatically increased the understanding of the important mechanistic features that apply to both the gas- and condensed-phase reactions.[3] The carefully controlled conditions now attainable for flowing afterglow studies allow one to examine gas-phase, bimolecular, ion–molecule reactions in which each partner is characterized by a 300 K energy. Reactive molecules or intermediates interacting with ions can often be more easily examined in the gas phase than in the liquid phase. With these recent experimental and theoretical advances, it is now becoming feasible to directly relate gas-phase ion–molecule results to similar reactions in condensed phase and vice versa. We recently have shown how the base-catalyzed decomposition of dimethyl disulfide (as a prototypical organic disulfide) could be readily examined in the gas phase.[4]

As part of our continuing interest in understanding the intrinsic reactivity of organic sulfur compounds, especially in relation to the utility of such functionality by bioorganic systems and in relation to the fate of sulfur in the atmosphere, we report here the first detailed anion–molecule studies of dimethyl sulfite (I). The related molecule dimethyl carbonate, $CH_3OCO_2CH_3$, has been briefly examined by the ion cyclotron resonance (ICR) and flowing afterglow (FA) techniques[5] and has been found to undergo nucleophilic attack at both sp^2 C and sp^3 C.

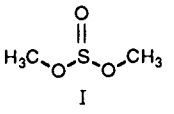

I

In this flowing afterglow study, we report the products observed and our mechanistic interpretations of a carefully selected series of anions interacting with dimethyl sulfite at 300 K, under reaction conditions designed to reveal the intrinsic chemical reactivity due to the anion and neutral alone, unperturbed by such mitigating factors as general and specific solvation, ion pairing, or molecular aggregation. Following our studies of many of the same anions with dimethyl disulfide, we were interested in isolating the factors that define the site of reactivity (C or S) and the type of reaction (S_N2, E2, or $B_{AC}2$) that occurs. These studies focus on the intramolecular competitive chemical processes that can occur for any ion–neutral encounter and to a much lesser extent, the absolute rate of reaction.

Experimental Section

These experiments were carried out at ambient temperatures (~300 K) utilizing a flowing afterglow,[6] which has been described previously.[7] The total pressure in the reaction region was normally 0.30 Torr and was established by maintaining a constant volumetric flow rate of helium (~7.2 STP L min^{-1}) while utilizing the full pumping capacity of our mechanical booster pumping system (rated at 481 L s^{-1} for air at 0.5 Torr). Helium was typically 99% or more of the total gas present in the reaction region, the remainder being composed of various amounts of either the gases used as neutral reactant or the gases used to form the reagent ions. When utilized as the first-formed reactant ion, H_2N^- and CH_3O^- were generated by dissociative electron attachment to ammonia (partial pressure of 0.002 Torr) or methanol (partial pressure of less than 10^{-4} Torr) directly in the upstream portion of the flowing afterglow. Amide production was quite clean, typically contaminated by only small amounts of HO^- (m/z 17) and the cluster ion $H_2N^-[NH_3]$ (m/z 33).[8] Even under conditions optimized for H^- detection (which were significantly different than normal operating conditions of our quadrupole mass filter based detection system) little H^- was observed when generating amide. Methoxide generated from dissociative electron attachment to methanol was contaminated by small amounts of the methoxide–methanol cluster ions, $CH_3O^-[CH_3OH]$ (m/z 63) and $CH_3O^-[CH_3OH]_2$ (m/z 95). Hydroxide ion was cleanly generated in a two-step process initiated by dissociative electron capture of nitrous oxide to give the atomic oxygen anion, which was then allowed to abstract an H atom from high-purity methane (0.002 Torr each of N_2O and CH_4).[9] The carbanions and anilide were formed by exothermic proton transfer[10] from an appropriate neutral to amide (e.g., $H_2C{=}CHCH_2^-$ from $H_2C{=}CH{-}CH_3$; $C_6H_5^-$ from C_6H_6). Cyclohexadienide was generated from both 1,3- and 1,4-cyclohexadiene. Pentadienyl anion was formed from 1,3-pentadiene. In addition to electron impact ionization, CH_3O^- was formed by chemical reaction of amide ion with methanol, this procedure also led to the formation of large amounts of methoxide–methanol cluster ions leading us to preferentially use the direct ionization method mentioned above.[11] HS^- was formed from the fast, quantitative reaction of HO^- with CS_2 (eq 1).[12]

$$HO^- + CS_2 \rightarrow HS^- + OCS \qquad \Delta H_{rxn} = -48.7 \text{ kcal mol}^{-1} \quad (1)$$

Neutral reagents are added to the instrument by means of a dedicated glass vacuum system that allows for sample purification and for monitoring of the volumetric flow rate of neutral. Liquid samples are handled in round-bottomed flasks fit with high-vacuum stopcocks; each sample was subjected to several freeze–pump–thaw cycles to remove dissolved gases. Volumetric flow rates of neutrals were determined by measuring a pressure rise in a calibrated volume. The nature of each reaction was examined *qualitatively*, under pseudo-first-order conditions, at fixed reaction time, by taking a complete mass spectrum at each of several different concentrations of the neutral reagent. The *quantitative* branching ratios reported are those that eliminate any contributions from secondary reactions and were obtained from separate experiments as described below. The identities of the ion products were determined primarily from their mass-to-charge (m/z) ratios. For the reactions examined in this paper we were often aided by the distinctive M + 2 peak of sulfur-containing ions.[13,14] The neutral reaction products are not detected; those written are based on mass balance, analogy to known reactions, thermochemical considerations, and chemical sense. On occasion, we carried out specific experiments designed to provide additional structural information on one product ion or another.

Dimethyl sulfite (nominal molecular weight 110; bp^{760} = 126 °C) was obtained from Aldrich Chemical Co. as a gold label reagent (purity >99.7%) and used as received. The ^1H NMR spectrum (Bruker, 500 MHz) in $CDCl_3$ reveals no impurities. GC analysis (Perkin Elmer Model 990 with Porapak column at 200 °C) indicates the sample is at least 99% pure. Cyclopentadiene was obtained by cracking dicyclopentadiene immediately prior to use and was kept in a dry ice–acetone bath while employed. 1,4-Cyclohexadiene was distilled immediately prior to use. All other reagents were used as received from commercial suppliers.

(1) Van Woerden, H. F. *Chem. Rev.* **1963**, *63*, 557–571.
(2) Bristow, P. A.; Tillet, J. G. *J. Chem. Soc. C* **1968**, 684–687.
(3) Jorgensen, W. L.; Blake, J. F.; Madura, J. D.; Wierschke, S. D. In *Supercomputer Research in Chemistry and Chemical Engineering*; Jensen, K. F., Truhlar, D. G., Eds.; ACS Symposium Series 353; American Chemical Society: Washington, DC, 1987; Chapter 12.
(4) Grabowski, J. J.; Zhang, L. *J. Am. Chem. Soc.* **1989**, *111*, 1193–1203.
(5) (a) Takashima, K.; Riveros, J. M. *J. Am. Chem. Soc.* **1978**, *100*, 6128–6132. (b) Dottore, M. F.; Bowie, J. H. *J. Chem. Soc., Perkin Trans. 2* **1982**, 283–286. (c) McDonald, R. N.; Chowdhury, A. K. *J. Am. Chem. Soc.* **1983**, *105*, 7267–7271.
(6) (a) Ferguson, E. E.; Fehsenfeld, F. C.; Schmeltekopf, A. L. In *Advances in Atomic and Molecular Physics*; Bates, D. R., Estermann, I., Eds.; Academic Press: New York, 1969; Vol. 5, pp 1–56. (b) Fehsenfeld, F. C. *Int. J. Mass Spectrom. Ion Phys.* **1975**, *16*, 151–166. (c) Smith, D.; Adams, N. G. In *Gas Phase Ion Chemistry*; Bowers, M. T., Ed.; Academic Press: New York, 1979; Vol. 1, Chapter 1. (d) Graul, S. T.; Squires, R. R. *Mass Spectrom. Rev.* **1988**, *7*, 263–358.
(7) Grabowski, J. J.; Melly, S. J. *Int. J. Mass Spectrom. Ion Proc.* **1987**, *81*, 147–164.
(8) Some of our earlier spectra were contaminated by strong signals of HC_2^-, which was traced to impurities in our cylinder of electronic grade ammonia and which disappeared when a different ammonia supply was used.
(9) Bohme, D. K.; Fehsenfeld, F. C. *Can. J. Chem.* **1969**, *47*, 2717–2719.
(10) Lias, S. G.; Bartmess, J. E.; Liebman, J. F.; Holmes, J. L.; Levin, R. D.; Mallard, W. G. *J. Phys. Chem. Ref. Data* **1988**, *17*, Supplement 1.
(11) Direct ionization of 1,2-dimethoxyethane has also been reported as a good source of methoxide ion: Jones, M. E.; Ellison, G. B. *J. Am. Chem. Soc.* **1989**, *111*, 1645–1654.
(12) Bierbaum, V. M.; Grabowski, J. J.; DePuy, C. H. *J. Phys. Chem.* **1984**, *88*, 1389–1393.
(13) The natural abundances of the sulfur isotopes are: 95.02% ^{32}S, 0.75% ^{33}S, 4.21% ^{34}S and 0.02% ^{36}S; ref 14.
(14) de Bievre, P.; Barnes, I. L. *Int. J. Mass Spectrom. Ion Phys.* **1985**, *65*, 211–230.

Table I. Summary of Results for the Quantitative Investigations of the Reactions of Anions with Dimethyl Sulfite in the Gas Phase at 300 K and 0.30 Torr of Helium

anion, A^- (parent)[a]	$\Delta H°_{acid}[AH]$,[b] kcal mol^{-1}	product ion, m/z	obsd amounts[c]	n_{BR}[d]	mol formula	isotope[e] factor	product[f] yields, %	$k_{total} \pm 1\sigma$[g] [Eff][h] (n_k)[d]
H_2N^- (ammonia)	403.7	62	0.055 ± 0.009	3	$(NOS)^-$	0.9444	5.4	4.52 ± 0.92 [1] (6)
		64	0.053 ± 0.010		$(O_2S)^-$	0.9457	5.2	
		79	0.437 ± 0.049		$(CH_3O_2S)^-$	0.9349	43.7	
		94	0.019 ± 0.001		$(CH_4NO_2S)^-$	0.9317	1.9	
		95	0.436 ± 0.062		$(CH_3O_3S)^-$	0.9326	43.8	
$C_6H_5^-$[i] (benzene)	400.8	64	0.005 ± 0.007	2	$(O_2S)^-$	0.9457	0.5	
		79	0.096 ± 0.008		$(CH_3O_2S)^-$	0.9349	9.5	
		95	0.787 ± 0.035		$(CH_3O_3S)^-$	0.9326	78.3	
		141	0.112 ± 0.018		$(C_6H_5O_2S)^-$	0.8843	11.7	
$H_3CSCH_2^-$[i] (dimethyl sulfide)	393.2	64	trace[j]	3[k]	$(O_2S)^-$	0.9457	trace[j]	
		79	0.004 ± 0.004		$(CH_3O_2S)^-$	0.9349	0.4	
		95	0.626 ± 0.013		$(CH_3O_3S)^-$	0.9326	61.2	
		107	0.320 ± 0.017		$(C_2H_3OS_2)^-$	0.8806	33.1	
		139	0.050 ± 0.004		$(C_3H_7O_2S_2)^-$	0.8683	5.3	
$H_2C{=}CHCH_2^-$ (propene)	390.8	87	0.526 ± 0.027	2	$(C_3H_3OS)^-$	0.9166	53.0	1.52 ± 0.12 [0.50] (2)
		95	0.441 ± 0.026		$(CH_3O_3S)^-$	0.9326	43.6	
		119	0.033 ± 0.001		$(C_4H_7O_2S)^-$	0.9038	3.4	
HO^- (water)	390.8	64	0.012 ± 0.015	3	$(O_2S)^-$	0.9457	1.2	2.43 ± 0.12 [0.72] (2)
		79	0.183 ± 0.006		$(CH_3O_2S)^-$	0.9349	18.3	
		95	0.805 ± 0.014		$(CH_3O_3S)^-$	0.9326	80.5	
$C_4H_3O^-$ (furan)	388[l]	95	0.543 ± 0.009	2	$(CH_3O_3S)^-$	0.9326	53.2	
		131	0.049 ± 0.026		$(C_4H_3O_3S)^-$	0.9022	5.0	
		145	0.408 ± 0.039		$(C_2H_5O_3S)^-$	0.8920	41.8	
$C_6H_5CH_2^-$ (toluene)	380.7	95	0.131 ± 0.036	2	$(CH_3O_3S)^-$	0.9326	12.3	0.656 ± 0.080 [0.28] (2)
		137	0.436 ± 0.017		$(C_7H_5OS)^-$	0.8767	43.7	
		169	0.433 ± 0.053		$(C_8H_9O_2S)^-$	0.8644	44.0	
CH_3O^- (methanol)	380.5	95	1.000		$(CH_3O_3S)^-$	0.9326	100	2.24 ± 0.086 [0.70] (3)
CD_3O^- (methanol-d_3)	381.0[m]	95	0.832 ± 0.005	2	$(CH_3O_3S)^-$	0.9326	83.2	
		98	0.168 ± 0.005		$(CD_3O_3S)^-$	0.9331	16.8	
$H_2C{=}CHCH{=}CHCH_2^-$ (1,3-pentadiene)	368.5	95	0.939 ± 0.003	2	$(CH_3O_3S)^-$	0.9326	93.6	0.0057 ± 0.005 [0.0023] (2)
		113	0.018 ± 0.001		$(C_5H_5OS)^-$	0.8963	1.9	
		145	0.043 ± 0.002		$(C_6H_9O_2S)^-$	0.8838	4.5	
HS^- (hydrogen sulfide)	351.1	95	0.984 ± 0.015	2	$(CH_3O_3S)^-$	0.9326	98.3	
		143	0.016 ± 0.018		$(C_2H_7O_3S_2)^-$	0.8759	1.7	

[a] The conjugate acid of this anion. [b] See ref 10 for source of gas-phase acidities. Error bars are quoted in the text. [c] The average fractional yield ± 1 standard deviation based on observation of only the m/z values listed for that reaction. [d] The number of independent experimental determinations of the branching ratio (BR) or rate coefficient (k). [e] The fraction of the product ion with the given molecular formula that will be detected at the m/z value listed (which is the predominant isotopic peak). These values were calculated from values in the Table of the Isotopes in ref 14. [f] The yield of the product ion of given molecular formula actually formed in the reaction cited (i.e., corrected to include all naturally occurring isotopic variants and any possible overlap of ions of different formula but identical nominal mass). These values are calculated by taking the "observed amounts" and dividing them by the "isotope factor" (and when necessary, subtracting for overlap) and then renormalizing. [g] Reaction rate in units of 10^{-9} cm^3 molecule^{-1} s^{-1}. [h] Reaction efficiency, $k_{obs}/k_{collision}$ where $k_{collision}$ is calculated according to ref 19. [i] See ref 24. [j] By trace, we mean <0.1% of the overall product ion yield, but the ion is consistently detected as a product of the listed ion–molecule reaction. [k] Includes one measurement at 0.5 Torr total pressure (see text). [l] Reference 25. [m] CD_3O^- has been observed to be 0.47 kcal mol^{-1} stronger a base than CH_3O^-.[26]

Branching ratios were obtained by monitoring the reactant and product ions involved in an ion–molecule reaction as a function of the extent of reaction. As described previously,[4] we find it most convenient to fix the reaction time and to vary the extent of reaction by changing the amount of neutral reagent present (always keeping within the constraint of the pseudo-first-order approximation). For such a situation, and where secondary reactions can be safely neglected, the amount of a product ion at time t is some fraction of the amount of reactant ion that has been consumed; this fraction, as is shown in eq 2 for A^- reacting with

$$[P_x^-]_t = \frac{k_x}{\Sigma k_x}\{[A^-]_0 - [A^-]_t\} \qquad (2)$$

a neutral by parallel pathways to give several product ions, P_x^-, is defined by the ratio of the rate cofficient for the single reaction channel of interest to the rate coefficient for disappearance of the reactant ion. In eq 2, $[P_x^-]_t$ is the amount of product ion X at point t in the reaction, k_x is the rate coefficient for producing product X^-, Σk_x is the total rate coefficient for disappearance of reactant ion (and which is equal to the sum of the individual rate coefficients for the parallel pathways) and $\{[A^-]_0 - [A^-]_t\}$ is the amount of reactant ion that has been consumed. By plotting the normalized ion intensities on the ordinate versus the amount of reactant ion that has been consumed by chemical reaction on the abscissa, we obtain a straight line, the slope of which is the branching ratio (i.e., the relative rate coefficient, $k_x/\Sigma k_x$) for that channel. Examples of such plots are shown in the Results. Combination of the relative rate coefficients so obtained with the absolute rate coefficient measured for the disappearance of reactant ion (discussed below) can give the absolute rate coefficient for each product-forming channel. For ion–molecule systems that show secondary reactions, where secondary processes are defined as the interaction of a product ion from the initial reaction with another molecule of the neutral reagent, the above plots yield curves that approach linearity at low conversions and that sharply deviate from linearity at high conversions. A quantitative analysis thus gives the primary product ion yields free from any contributions due to secondary reactions (slopes from the linear portion of the curve) and at least qualitative information on any reasonably fast secondary reactions (from the shapes of the curves at high conversions). The primary product ion yields can be considered to be the probability of following a given channel from a single ion–molecule collision complex (and neglecting the nonproductive process leading back to separated reactants).

For all reactions examined, we find a branching ratio analysis yields extremely good fits to the linear model discussed above. Our quantitative measurements are listed in Table I, each of which is the average of a minimum of duplicate experiments (see column 5, Table I). Typically we find that we can repeat measurements to a few tenths of a percent if the experiments are done one immediately following the other. The absolute reproducibility is several percentage points (for examples, see Table I) if experiments are repeated with an intervening time period of several weeks. We feel that the major systematic error is our inability to accurately retune the mass programmer[15] between experiments to the

top of the individual mass peaks that are quantitatively monitored during an experiment. Hence, back-to-back measurements reduce apparent deviations between experiments but may hide small, but significant, deviations between observed measurements and the true values. For this reason, we execute repeated measurements on separate days such that a complete retuning of the mass programmer is mandated. We plan to implement an extensive computer-driven data collection process utilizing a dynamic mass programmer that will obviate the need of a static mass programmer.

Branching ratios are experimentally determined by monitoring the most intense isotopic mass spectral peak for any given ion. The predominant isotope of sulfur has an atomic weight of 32 amu (95.02% of naturally occurring sulfur) with significant populations at 33 amu (0.75%) and 34 amu (4.21%).[13,14] Thus by monitoring only the most intense peak for a sulfur-containing ion, we miss a minimum of 4.96% of that ion. The other elements also have populations distributed over different isotopic forms. We take into account the distribution of any given ionic molecular formula over a range of mass-to-charge values, by experimentally monitoring the most abundant isotopic peak and then multiplying that observed ion yield by the necessary correction factor computed from standard isotope tables.[14] Such isotopic correction factors are included in Table I.

While the measurement of rate coefficients is not the focus of this work, several such measurements are included in Table I, each value of which is the average of at least two independent measurements. All such measurements are obtained by quantitatively monitoring the decrease in reactant ion signal (e.g., A^-) at a fixed reaction distance (and hence time), as the amount of neutral reagent is changed while maintaining the limits defined by the pseudo-first-order kinetic approximation (or by varying reaction distance at a fixed neutral concentration). The slope of the semilogarithmic plot of decay of reactant ion versus concentration of neutral reagent yields the observed, absolute, bimolecular rate coefficient (k_{obs}) according to the expression shown in eq 3, which is analo-

$$k_{obs} = \frac{\Delta \ln [A^-]}{\Delta(F_{neutral})} \frac{F_{He}^2 T^2}{P_{He}^2 z}\{1.10 \times 10^{-20}\} \quad (3)$$

gous to that derived previously.[6d,16] In eq 3, F_{He} is the volumetric flow rate of helium buffer gas (in STP $cm^3\ s^{-1}$), P_{He} is the average flow-tube pressure throughout the reaction region (in Torr), T is the ambient temperature (in K), z is the physical distance between the point of neutral addition and point of ion detection (in cm),[17] $F_{neutral}$ is the volumetric flow rate of the neutral (in STP $cm^3\ s^{-1}$). The constant in eq 3 contains all the necessary unit conversion parameters as well as α, which we assume to be 1.60 (i.e., α, the average ion velocity,[6a,18] is 1.60 times the average neutral velocity). Due to the number of approximations used in deriving eq 3 and the rather small number of independent measurements of a single rate coefficient, we feel that the error bars on the reported rate coefficients should be considered to be about 40% (which is about twice the normal error limit quoted for rate coefficients determined by the FA technique). Because many gas-phase ion–molecule reactions are fast, occurring on a high percentage of the thermal collisions, and since the collision rate depends on the exact ion and neutral involved, we prefer to discuss reaction efficiencies (the numbers in brackets in the final column of Table I) rather than absolute reaction rates. Reaction efficiencies (Eff), defined as the fraction of collisions that give rise to products, are obtained by dividing the observed bimolecular rate coefficient by the collision rate coefficient, which is calculated according to the parametrized trajectory theory of Su and Chesnavich[19] using a dipole moment[20] of 2.93 D for dimethyl sulfite and a polarizability of 9.3×10^{-24} cm^3 obtained as the average of values derived from the index of refraction[21] and group additivity.[22]

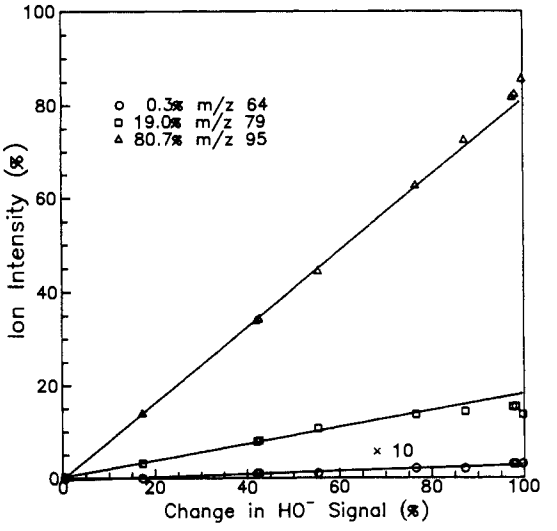

Figure 1. Typical branching ratio plot observed for the reaction of HO^- and $CH_3OSO_2CH_3$ in 0.30 Torr of helium at 300 K. Note that, for clarity, the m/z 64 data is displayed at 10 times its actual yield. The downward curvature in the m/z 79 data and the upward curvature in the m/z 95 data indicate a secondary reaction, which converts the m/z 79 into m/z 95 upon reaction with a second molecule of dimethyl sulfite. The solid lines drawn are those defined by eq 2 and are fitted to the data which correspond to less than 80% conversion. The observed amounts of the three product ions (the slopes of the fitted lines) are shown in the legend.

Results

The results of our quantitative measurements are summarized in Table I, in which the data are listed in order of decreasing Brønsted base strength (column 2) of the nucleophile examined (column 1). $\Delta H°_{acid}(AH)$ is the enthalpy of the gas-phase heterolytic dissociation of acid AH to A^- and H^+ and has the same absolute value as the proton affinity of the conjugate base, $PA(A^-)$; thus in this manuscript we use "acidity" when referring to proton loss from neutrals and "proton affinity" when discussing proton gain by anions. Columns three and four list each product ion monitored for a given reaction and the directly observed amount of each mass-to-charge ratio. Table I also includes the number of independent experiments performed for each branching ratio reported (column 5), the molecular formula deduced for the product ion (column 6), the factor used to correct the observed data to include all naturally occurring isotopic variants as discussed above (column 7), and the product yield (column 8) of each chemically distinct species. The final column in Table I contains the observed bimolecular rate coefficient (±1 standard deviation), the reaction efficiency (the number in brackets), and the number of independent measurements on which it is based (the number in parentheses) for those nucleophiles for which we made such measurements. In addition to the quantitative data in Table I, further comments and observations are presented in the next

(15) A mass programmer is an electronic device that directs the quadrupole mass filter to pass one mass-to-charge ratio at a time but that contains eight independent channels, which must be reset before each experiment. Thus up to eight mass-to-charge ratios can be repetitively monitored with a high accuracy of returning to the exact same portion of the ion peak. Such a device is indispensable for obtaining our branching ratio data.

(16) Bierbaum, V. M.; DePuy, C. H.; Shapiro, R. H.; Stewart, J. H. *J. Am. Chem. Soc.* **1976**, *98*, 4229–4235.

(17) We have not corrected the physical reaction distance for any end (mixing) effects. Due to the simple design of our neutral addition port (a 0.10-cm-diameter opening at the flow-tube wall), we expect a positive end effect such that the actual reaction distance will be somewhat smaller than the physical distance. Adoption of such a correction will cause a modest increase in our reported rate coefficients. Some of the kinetic data were obtained with a "kinetics tube", which was installed toward the end of this work and which contains 10, equally spaced, identical, radial inlets (McFarland, M.; Albritton, D. L.; Fehsenfeld, F. C.; Ferguson, E. E.; Schmeltekopf, A. L. *J. Chem. Phys.* **1973**, *59*, 6610–6619). The rate coefficients obtained by varying the reaction distance are independent of end effects and are found to be within 1 standard deviation of the values obtained by varying the neutral flow at constant reaction distance (and hence time).

(18) (a) Huggins, R. W.; Cahn, J. H. *J. Appl. Phys.* **1967**, *38*, 180–188. (b) Cher, M.; Hollingsworth, C. S. In *Chemical Reactions in Electrical Discharges*; Gould, R. F., Ed.; Advances in Chemistry Series 80, American Chemical Society: Washington, DC, 1969; pp 118–132. (c) Stock, H. M. P. *J. Phys. B* **1973**, *6*, L86–L88. (d) Upschulte, B. L.; Shul, R. J.; Passarella, R.; Keesee, R. G.; Castleman, A. W. *Int. J. Mass Spectrom. Ion Proc.* **1987**, *75*, 27–45.

(19) Su, T.; Chesnavich, W. J. *J. Chem. Phys.* **1982**, *76*, 5183–5185.

(20) McClellan, A. L. *Tables of Experimental Dipole Moments*; W. H. Freeman and Co.: San Francisco, 1963.

(21) Using η = 1.4096 in the Lorentz–Lorenz relation cited in: Shoemaker, D. P.; Garland, C. W.; Steinfeld, J. I.; Nibler, J. W. *Experiments in Physical Chemistry*, 4th ed.; McGraw Hill: New York, 1981; p 383.

(22) Miller, K. J.; Savchik, J. A. *J. Am. Chem. Soc.* **1979**, *101*, 7206–7213.

section for those reactions present in Table I as well as for other reactions, which formed only a single product ion or reactions for which no quantitative data were taken.

To determine how reliably we can actually measure relative ion intensities, we made M and M + 2 measurements on the m/z 95 product ion generated from HS^-, one of the nucleophiles examined in this study. For these measurements we set the quadrupole resolution to the minimum value that gives base-line separation between two adjacent peaks up to $m/z \sim 500$ (i.e., our typical operating conditions in which fwhm is slightly smaller than 1 amu). The relative intensities of m/z 95 to m/z 97 observed are 1.0000:0.0563 in reasonable agreement with that expected[14] of 1.0000:0.0517 for a molecular formula of CH_3O_3S. On the basis of such measurements our accuracy is probably ±0.4% on any individual branching ratio measurement.

Hydroxide ($PA[HO^-] = 390.8 \pm 0.1$ kcal mol^{-1}) is not the most basic anion that we examined but rather is the first we must discuss since hydroxide is an impurity ion present in the reactant ion spectra of all anions of higher proton affinity than hydroxide. When hydroxide reacts with dimethyl sulfite, under the thermally equilibrated conditions in the FA, a rapid reaction occurs ($k_{obs} = 2.4 \times 10^{-9}$ cm^3 molecule^{-1} s^{-1}; Eff = 0.72) giving principally an ion at m/z 95, considerably less of m/z 79, and a minor amount of m/z 64, as shown in Table I. The "M + 2" isotopic peak detected for each of these three ions indicates the presence of a single sulfur atom for all product ions. An example of one of the three quantitative branching ratios obtained for this reaction is shown in Figure 1. Examination of Figure 1 shows that the data appear to be quite linear at less than 80% conversion and from which we obtain the single individual measurement shown in the legend of Figure 1, while the average of three independent experiments is shown in Table I. As an example of the reproducibility of our branching ratio measurements, we include here the three separate branching ratios that were averaged to give the values in column 4 of Table I: m/z 64, 2.9%, 0.3%, 0.4%; m/z 79, 18.0%, 19.0%, 17.9%; m/z 95, 79.1%, 80.7%, 81.7%. The curvature noted at high conversions in Figure 1 combined with the qualitative spectra taken for this reaction (not shown) indicates that the m/z 79 primary product ion reacts with a second equivalent of dimethyl sulfite to give m/z 95 (i.e., no product ions other than m/z 64, 79, and 95 are detected at the higher conversions indicated by the right-hand portion of Figure 1). Note that m/z 64 remains inert to further reaction with dimethyl sulfite under the reaction conditions necessary to completely quench HO^-.

Amide ($PA[H_2N^-] = 403.7 \pm 0.8$ kcal mol^{-1}) reacts rapidly with dimethyl sulfite ($k_{obs} = 4.5 \times 10^{-9}$ cm^3 molecule^{-1} s^{-1}; Eff = 1) to give the five product ions shown in Table I. From an examination of only the qualitative mass spectra, it is apparent that m/z 79 and 95 are formed in similar yields and that m/z 79 undergoes a facile secondary reaction, which also produces m/z 95. The secondary reaction is sufficiently fast enough to allow us to completely quench the m/z 79 product ion. In order to obtain an accurate branching ratio, we must also take into account the small amount of hydroxide that is present in our amide ion reactant spectrum (the average amide to hydroxide ratio was 6.4:1) and that displays its own rapid reaction with dimethyl sulfite (vide supra). The correction was done within each amide ion branching ratio measurement, on a point-by-point basis as described by eq 4.[23] In eq 4, $[P_x^-]_{corr}$ is the yield of product ion x due solely to

$$[P_x^-]_{corr} = [P_x^-]_{obs} - \{[HO^-]_0 - [HO^-]_{obs}\}BR(P_x^-) \quad (4)$$

amide reaction, $[P_x^-]_{obs}$ is the experimentally observed yield of product ion x and which may have arisen from both amide and hydroxide reactant ions, $[HO^-]_0$ is the initial amount of hydroxide present in the amide reactant ion spectrum, $[HO^-]_{obs}$ is the amount of hydroxide remaining, and $BR(P_x^-)$ is the branching ratio (relative yield) of product ion x from the known hydroxide reaction (discussed above). An example of a corrected branching ratio plot is shown in Figure 2. A semiquantitative estimate of the branching ratio for this reaction at a flow-tube pressure of 0.50 Torr of helium reveals no significant changes from the results reported for 0.30 Torr of helium.

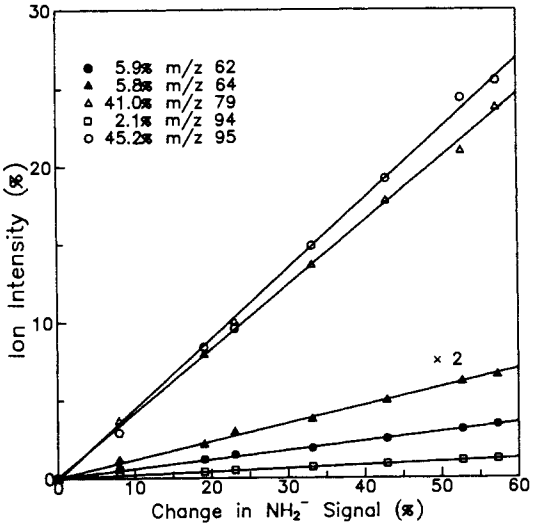

Figure 2. Typical branching ratio plot observed for the reaction of H_2N^- and $CH_3OSO_2CH_3$ in 0.30 Torr of helium at 300 K. For clarity, the m/z 64 data are shown at twice their actual intensity. Note that the observed data for this reaction has been corrected to remove contributions due to HO^- impurity in the reactant ion signal, as discussed in the text; the corrected data are shown. The downward curvature in the m/z 79 data and the upward curvature in the m/z 95 data expected at high conversions, based on the data presented in Figure 1, are not observed here because the reaction was only followed to 60% conversion of the initial amide signal. The curvature due to the secondary reaction is readily observed when the amide reaction is monitored to greater than 80% conversion. The solid lines drawn are those defined by eq 2, the slopes of which give the observed amounts of the five product ions shown in the legend.

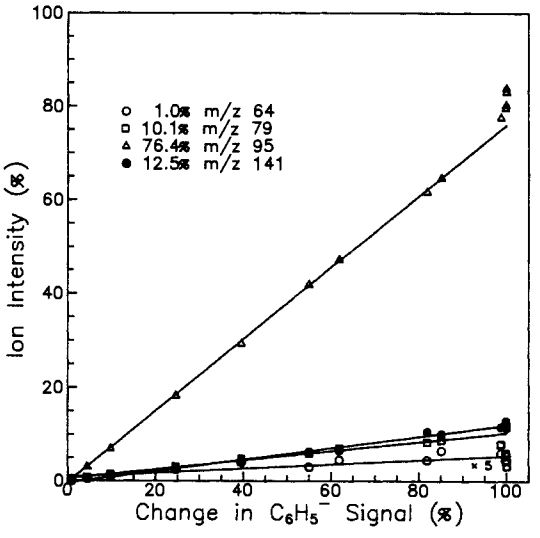

Figure 3. Typical branching ratio plot observed for the reaction of phenide ion with dimethyl sulfite in 0.30 Torr of helium at 300 K. The existence of the facile secondary reaction (the further conversion of m/z 79 to m/z 95 upon reaction with a second equivalent of dimethyl sulfite) is readily apparent in the right-hand portion of the data plot. Note that both m/z 64 (displayed at 5 times its actual value) and m/z 141 are inert to further reaction with dimethyl sulfite under these conditions. The solid lines drawn are those defined by eq 2 and fitted to the data which correspond to less than 90% conversion of the initial phenide ion concentration. The observed amounts of the four product ions reported in the legend are from the slopes of the lines.

(23) If one simply neglects the hydroxide, the observed amounts of products for amide with dimethyl sulfite (averaged over the three independent branching ratio measurements) are the following: 4.5 ± 0.5%, m/z 62, 4.6 ± 0.6%, m/z 64, 40.4 ± 4.7%, m/z 79, 1.8 ± 0.2%, m/z 94, 48.7 ± 5.4%, m/z 95. Comparing this latter branching ratio with that reported in Table I, which has been corrected for hydroxide contamination of the reactant ion spectrum, shows that the overall correction is small.

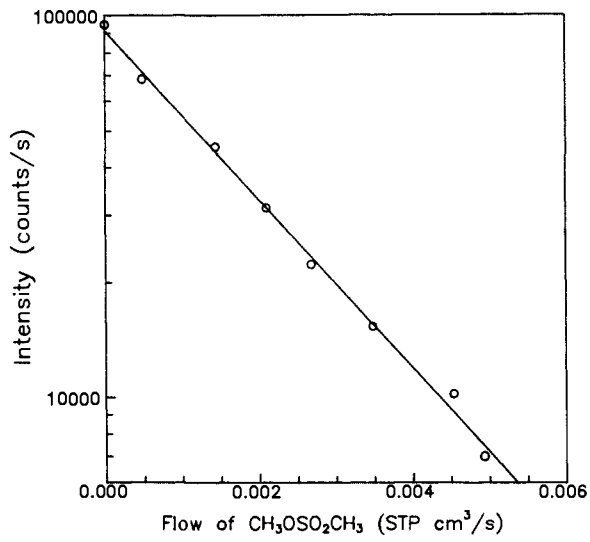

Figure 4. Semilog plot of observed allyl ion intensity as a function of dimethyl sulfite concentration at constant reaction time. The slope of this plot (R = 0.998; error in slope is 2.4%) in combination with eq 3 gives a rate coefficient of 1.60×10^{-9} cm^3 $molecule^{-1}$ s^{-1} for this one measurement. This plot corresponds to following the allyl anion concentration for about 4 half-lives.

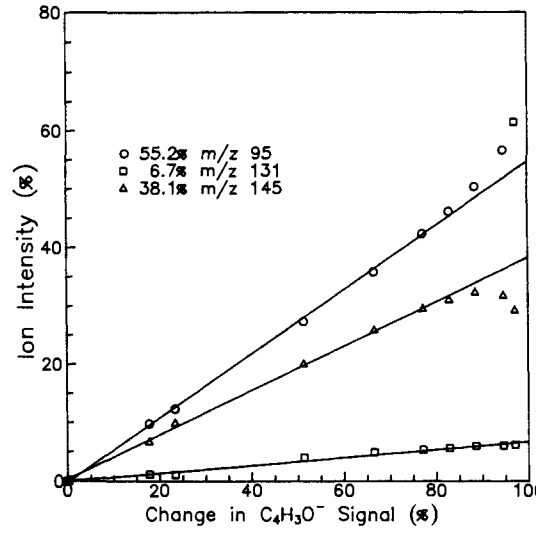

Figure 5. One of the duplicate measurements used to quantify the branching ratio exhibited by the reaction of the conjugate base of furan with dimethyl sulfite in 0.30 Torr of helium at 300 K. The observed amounts of the three primary product ions (shown in the legend) are obtained from eq 2 and the data corresponding to less than 80% conversion of the initial $C_4H_3O^-$ signal. At higher conversions, the existence of a facile secondary reaction is noted in which the m/z 145 ion undergoes a reaction with dimethyl sulfite to form additional m/z 95. No new ions are observed in the mass spectrum at these higher conversion conditions.

Phenide[24] ($PA[C_6H_5^-]$ = 400.8 ± 0.5 kcal mol^{-1}) undergoes rapid reaction with dimethyl sulfite to give principally m/z 95 ion, lesser amounts of m/z 141 and 79, and just a minor amount of m/z 64. Inspection of the "M + 2" isotopic peaks reveals that all four product ions from this reaction contain a sulfur atom. As is true for both hydroxide and amide ions, the initial m/z 79 product ion undergoes a facile secondary reaction with another molecule of the sulfite to give exclusively a m/z 95 ion. The secondary reaction is readily apparent in the example of the branching ratio plot shown in Figure 3.

The conjugate base of dimethyl sulfide[24] ($PA[CH_3SCH_2^-]$ = 393.2 ± 2.6 kcal mol^{-1}) produces four distinct product ions in a fast reaction with dimethyl sulfite, among which m/z 95 followed by m/z 107 is most abundant. We also detect trace amounts of m/z 64, but at such low abundances that we can only reliably state that it is a trace product that accounts for less than 0.1% of all product ions for this reaction. Two independent measurements of the branching ratio, at a flow-tube pressure of 0.30 Torr, gave the following quantitated amounts: 0.003, m/z 79; 0.623, m/z 95; 0.326, m/z 107; 0.048, m/z 139. A third measurement at a flow-tube pressure of 0.50 Torr gave the following: 0.009, m/z 79; 0.634, m/z 95; 0.301, m/z 107; 0.056, m/z 139. Since there is no difference between the measurements made at the two flow-tube pressures, the combined average of these three measurements is reported in Table I.

Allyl anion ($PA[H_2C{=}CHCH_2^-]$ = 390.8 ± 2.4 kcal mol^{-1}) also undergoes a facile reaction with dimethyl sulfite (k_{obs} = 1.5×10^{-9} cm^3 $molecule^{-1}$ s^{-1}; Eff = 0.50), giving m/z 87 as the major product ion, followed by a lesser amount of m/z 95 and a minor amount of m/z 119. The branching ratio plots for this reaction indicate that there are no secondary reactions occurring during the time it takes to completely quench the allyl anion signal. All three product ions contain a sulfur atom as evidenced by their M + 2 isotopic peaks. An example of the data used to obtain the rate coefficient for this reaction is shown in Figure 4.

The conjugate base of furan ($PA[C_4H_3O^-]$ = 388 ± 3 kcal mol^{-1})[25] readily reacts with dimethyl sulfite. The major product ion is m/z 95, with a lesser amount of m/z 145 formed as well as a minor amount of m/z 131. All three product ions display the M + 2 isotopic peak characteristic of the presence of a single sulfur atom. One of the duplicate measurements of this branching ratio is shown in Figure 5. From the behavior of the data displayed in Figure 5 and the observation that even under reaction conditions well beyond those needed to quench the initial reactant ion, no additional product ions are found; it is apparent that the m/z 145 product ion reacts with a second dimethyl sulfite molecule to give only m/z 95.

The benzyl anion ($PA[C_6H_5CH_2^-]$ = 380.7 ± 2.4 kcal mol^{-1}) undergoes a fast reaction with dimethyl sulfite (k_{obs} = 6.6×10^{-10} cm^3 $molecule^{-1}$ s^{-1}, Eff = 0.28). Three product ions, each bearing a sulfur atom, are formed from the interaction of benzyl anion with dimethyl sulfite, all three are of significant yield (Table I), and all three appear to be stable against further reaction under the conditions necessary to allow complete reaction of the initial nucleophile.

Methoxide ($PA[CH_3O^-]$ = 380.5 ± 2.2 kcal mol^{-1}) undergoes an efficient reaction with dimethyl sulfite (k_{obs} = 2.2×10^{-9} cm^3 $molecule^{-1}$ s^{-1}; Eff = 0.70) giving as a single product, the m/z 95 ion. When the methoxide was labeled with deuterium ($PA[CD_3O^-]$ = 381.0 ± 2.4 kcal mol^{-1}),[26] a new pathway was revealed in which an ion at m/z 98 is formed (containing a single sulfur atom). No CH_3O^- was detected in the reaction of CD_3O^- with dimethyl sulfite. The quantitative data are summarized in Table I while one of the duplicate measurements of the CD_3O^- branching ratio is shown in Figure 6. The curves remained linear even up to 94% conversion of CD_3O^-.

Cyclohexadienide ($PA[c\text{-}C_6H_7^-]$ = 373.3 ± 5.0 kcal mol^{-1}) is observed to give three products in qualitative experiments.[27] The principle product ion, about 60% of the reaction products, appears at m/z 95 ($CH_3O_3S^-$); approximately 15% of the reaction gives products at m/z 157 ($C_7H_9O_2S^-$), and the remaining 25% of the

(24) The data reported in Table I and discussed in the text for the reactions of phenide and the conjugate base of dimethyl sulfide have not been corrected for contributions due to the small amount of hydroxide ion present, due to technical complications during the collection of these data. On the basis of the correction for the hydroxide in the amide experiment,[23] we expect that such a correction for the two cases under discussion would result in less than 2% changes in the reported product yields.

(25) DePuy, C. H.; Kass, S. R.; Bean, G. P. *J. Org. Chem.* **1988**, *53*, 4427–4433.

(26) On the basis of the gas-phase acidity of methanol cited in ref 10 and the 0.5 kcal/mol difference between methanol and methanol-d_3 cited in: Grabowski, J. J.; DePuy, C. H.; Van Doren, J. M.; Bierbaum, V. M. *J. Am. Chem. Soc.* **1985**, *107*, 7384–7389.

(27) The qualitative product ion yields cited are estimated from peak heights measured by a ruler from mass spectral plots and should be accurate to ca. ±7% (i.e., a 60% yield is really known to be somewhere between 53 and 67%).

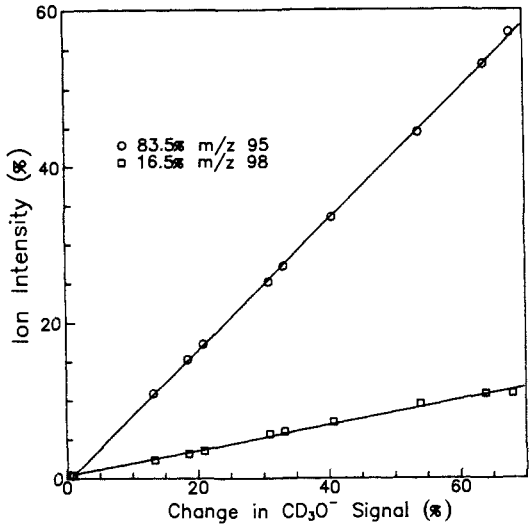

Figure 6. A branching ratio measurement for the reaction of CD_3O^- with $CH_3OSO_2CH_3$ in 0.30 Torr of helium at 300 K. No change in the product ion composition is observed in this system even under conditions well beyond those needed to quench methoxide, indicating that neither m/z 95 nor 98 react again with dimethyl sulfite. The solid lines represent fits of the observed data points to eq 2 and which yield the observed amounts shown in the legend.

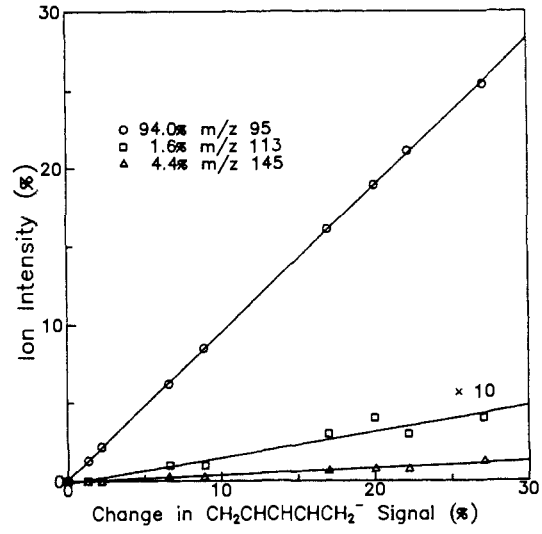

Figure 7. Typical branching ratio plot observed for the reaction of pentadienyl anion and $CH_3OSO_2CH_3$ in 0.30 Torr of helium at 300 K. The intensity of the m/z 113 product ion is shown at 10 times its actual value for clarity. Due to the slowness of this reaction and the low volatility of dimethyl sulfite, 30% conversion, based on the initial pentadienyl anion signal, was the most that could be achieved. The solid lines drawn are those defined by eq 2, the slopes of which are used to obtain the observed amounts reported in the legend.

products appear at m/z 125 ($C_6H_5OS^-$). The M + 2 isotopic peaks of the three product ions indicate that all contain a single sulfur atom. The reaction can be considered to be moderately slow.[28] No secondary reactions were observed.

Cyanomethide ($PA[H_2CCN^-]$ = 372.8 ± 2.6 kcal mol^{-1}), in qualitative experiments, is observed to undergo moderately fast reaction with dimethyl sulfite, giving predominantly, if not exclusively, the m/z 95 product ion. It is likely that the trace amount of adduct ion observed at m/z 136 is the product of a termolecular reaction of the m/z 95 product ion clustering with acetonitrile (which is present in fairly high concentrations).

Pentadienyl anion ($PA[C_5H_7^-]$ = 368.5 ± 3.6 kcal mol^{-1}) gave a rather slow reaction (k_{obs} = 5.7 × 10^{-12} cm^3 molecule^{-1} s^{-1}; Eff = 0.0023) with dimethyl sulfite. The combination of the low rate coefficient and moderate vapor pressure of dimethyl sulfite was such that we were unable to quench more than about 25% of the initial pentadienide signal. The predominant pathway exhibited produces m/z 95 while both m/z 145 and 113 are produced in minor amounts. A trace (≤0.1%) of the adduct ion at m/z 177 is observed at 0.30 Torr of helium and is believed to be a secondary product. All three primary product ions contain a sulfur atom. One of the duplicate measurements of the branching ratio for this reaction is shown in Figure 7; note that in contrast to the data shown in Figures 1–3, 5, and 6, the initial reactant ion signal is not even half-quenched.

Anilide ($PA[PhNH^-]$ = 366.4 ± 2.6 kcal mol^{-1}) was observed to react extremely slowly (as was found for the pentadienyl anion, the anilide reactant ion signal can only be partially quenched) with dimethyl sulfite to give principally the ion at m/z 95 ($CH_3O_3S^-$). In addition, a minor amount of the adduct ion, m/z 202, is also detected, but the precursor ion to it is unclear for the following reason. In a 0.30 Torr of helium bath gas, anilide ion undergoes efficient clustering with aniline to produce the anilide–aniline proton bound dimer, m/z 185. Under our experimental conditions, where we have added sufficient aniline to the initial amide ion signal to ensure that all amide (to less than 0.01% of the initial amount) has reacted prior to addition of dimethyl sulfite, we observe approximately equal amounts of anilide ion and the anilide–aniline cluster ion. The insignificant amount of observed cluster product ion at m/z 202 is believed to be formed by a "solvent-switching" reaction between the anilide–aniline cluster ion and dimethyl sulfite.

Acetaldehyde enolate ($PA[H_2C{=}CHO^-]$ = 365.9 ± 2.9 kcal mol^{-1}) undergoes a moderately rapid reaction in 0.30 Torr of helium bath gas (k_{obs} = 1.3 × 10^{-10} cm^3 molecule^{-1} s^{-1}; Eff = 0.046) with dimethyl sulfite to give two products. From qualitative height measurements[27] of recorded mass spectra, approximately 85% of the reaction proceeds to form the product ion at m/z 95 ($CH_3O_3S^-$) and the remaining 15% gives m/z 153 (which corresponds to the adduct or cluster ion). Unlike anilide and pentadienide discussed above, we are able to quench the enolate reactant ion signal. Since the yield of the m/z 153 clustered product ion is independent of the amount of the acetaldehyde enolate–acetaldehyde cluster ion in the reactant ion-only spectrum, we can rule out solvent-switching reactions as a source of the higher mass product ion. Thus the precursor ion to both product ions must be the enolate ion itself.

Nitromethide ($PA[H_2CNO_2^-]$ = 356.4 ± 2.9 kcal mol^{-1}) and **cyclopentadienide** ($PA[c\text{-}C_5H_5^-]$ = 354.0 ± 2.9 kcal mol^{-1}) undergo slow reaction to give only the corresponding adduct or cluster ion, m/z 170 and 175, respectively. Both of these (presumably termolecular) reactions are slow enough that we are unable to quench the reactant ion signal at 0.30 Torr total flow-tube pressure.

Hydrogen sulfide anion ($PA[HS^-]$ = 351.1 ± 2.2 kcal mol^{-1}), as shown in Figure 8, reacts slowly with dimethyl sulfite to produce two product ions, m/z 95 as the predominant ion and the cluster ion, m/z 143, as a minor component. Despite the reduced basicity of this anion as compared to some of those discussed above, we are able to just quench all the reactant ion signal within the experimental time window available to us. Also, since HS^- is synthesized via reaction of HO^- with carbon disulfide (eq 1), no $HS^-(H_2S)$ cluster is present, making it easy to confirm that both product ions observed result directly from reaction of HS^- with dimethyl sulfite.

Miscellaneous. In order to determine if the m/z 95 anion, to which we have assigned the structure of the ion resulting from S_N2 displacement at methyl in dimethyl sulfite, $CH_3OSO_2^-$, undergoes a self-regeneration reaction with dimethyl sulfite, we allowed the m/z 95 generated from hydroxide and dimethyl sulfite to react with ethyl methyl sulfite.[29] For this latter reaction, we

(28) Under our standard conditions, with a physical reaction distance of 56 cm, it was not possible to completely quench the final 10% or so of cyclohexadienide signal. The limiting factor for the lack of quenching is the relatively low vapor pressure of dimethyl sulfite.

(29) Lum, R. C.; Grabowski, J. J. *J. Am. Chem. Soc.* **1988**, *110*, 8568–8570.

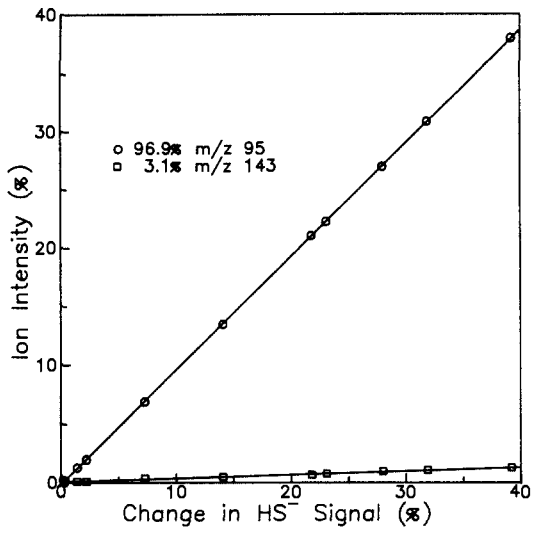

Figure 8. Branching ratio plot for the slow reaction of HS^- with dimethyl sulfite in 0.30 Torr of helium at 300 K. Even though this nucleophile is a relatively weak base, in other experiments, we are just able to quench all the reactant ion signal. Only two product ions are found as indicated in the figure, neither of which displays a secondary reaction with an additional molecule of dimethyl sulfite under any conditions attainable in the FA. The data, fit to eq 2, produce the observed amounts reported in the legend.

Table II. Summary of Results for the Qualitative Investigations of the Reactions of $CH_3OSO_2^-$ with Brønsted Acids

neutral	$\Delta H°_{acid}$,[a] kcal mol^{-1}	CH_3OSOO^- + neutral → ?
CD_3OD	381.0[b]	no reaction
CH_3COCH_3	369.0	no reaction
CH_3CONH_2	~362[c]	cluster formation only; $CH_3OSO_2^-(CH_3CONH_2)$
CF_3CH_2OH	361.8	cluster formation only; $CH_3OSO_2^-(CF_3CH_2OH)$
H_2S	351.1	no proton transfer; only formation of $HOSOS^-$
CH_3CO_2H	348.7	no proton transfer; only formation of $CH_3CO_2SO_2^-$
HCO_2H	345.1	no proton transfer; only formation of $HCO_2SO_2^-$
$CH_3COCH_2COCH_3$	343.7	minor proton transfer; major formation of $(CH_3CO)_2CHSO_2^-$
$ClCH_2CO_2H$	336.3	proton transfer and formation of $ClCH_2CO_2SO_2^-$
CF_3CO_2H	322.9	only proton transfer

[a] Unless noted, all acidities are obtained from ref 10. [b] Reference 26. [c] The acidity value listed for acetamide is actually that for *N*-methylacetamide and was obtained from ref 30.

were unable to observe generation of any product ion, and, specifically, no m/z 109 ($CH_3CH_2OSO_2^-$) was detected. This observation, in conjunction with the lack of curvature in the CD_3O^- plus $CH_3OSO_2CH_3$ branching ratio plots, confirms that the m/z 95 is unreactive toward dimethyl sulfite on the time scales utilized here.

Amide, the conjugate base of dimethyl sulfide, allyl anion, benzyl anion, and pentadienyl anion will react with dimethyl sulfite to yield products, which arise from loss of one or two molecules of methanol. Solvent-switching experiments with methanol-d_4, ethanol, trifluoroethanol, and water, carried out on the product mixtures produced from the noted nucleophiles, demonstrated that the one-methanol loss product (e.g., eq 12c, vide infra) is not a cluster ion. In order to at least roughly bracket the proton affinity of $CH_3OSO_2^-$ (i.e., the acidity of CH_3OSO_2H), we generated the m/z 95 anion by means of HO^- and dimethyl sulfite and then allowed it to react with the series of reagents listed in Table II. These data are discussed below. Table III sorts the data in Table I into a form that is more amenable to comparison and that depends somewhat on our interpretation discussed below. Table IV compiles the heats of formation used in this work.

Table III. Partitioning of Observed Product Ions among Available Reaction Pathways for the Interaction of Anions with Dimethyl Sulfite in 0.30 Torr of Helium at 300 K[a]

nucleophile	$\Delta H°_{acid}$,[b] kcal mol^{-1}	sulfur	carbon		adduct
			S_N2	E2	
H_2N^-	403.7	7.4	44.3	48.3	0
$C_6H_5^-$	400.8	11.7	78.3	10.0	0
$CH_3SCH_2^-$	393.2	38.4	61.2	0.4	0
$H_2C{=}CHCH_2^-$	390.8	56.4	43.6	0	0
HO^-	390.8		80.5[c]	19.5	0
c-$C_4H_3O^-$[d]	388	46.8	53.2	0	0
CD_3O^-[e]	381.0	50.4	49.6	0	0
$PhCH_2^-$	380.7	87.7	12.3	0	0
c-$C_6H_7^-$[f]	373.3	~40	~60	0	0
CH_2CN^-	372.8	0	~100	0	0
$H_2C{=}CHCH{=}CHCH_2^-$	368.5	6.4	93.6	0	0
$PhNH^-$	366.4	0	~100	0	0
$H_2C{=}CHO^-$	365.9	0	~85	0	~15
$H_2CNO_2^-$	356.4	0	0	0	100
c-$C_5H_5^-$[g]	354.0	0	0	0	100
HS^-	351.1	0	98.3	0	1.7

[a] See text and Table I for specific products observed. Yields indicated by approximate signs are from semiquantitative analysis of recorded mass spectra. The data have not been adjusted for the number of equivalent reaction sites in dimethyl sulfite. [b] Footnote *a* of Table I. [c] Without isotopic labeling of the hydroxide oxygen, we are unable to discern whether the observed product results from reaction at carbon or at sulfur. [d] Generated by proton abstraction by amide from furan. [e] Yield of products resulting from sulfur versus carbon attack is based on the model discussed in the text. [f] Generated by proton abstraction from cyclohexadiene. [g] Generated by proton abstraction from cyclopentadiene.

Table IV. Heats of Formation Used in This Work

neutral	$\Delta H_f°_{298}$, kcal mol^{-1}	ref	anion	$\Delta H_f°_{298}$, kcal mol^{-1}	ref
CH_3	+34.8	*a*			
NH_3	−11.0	*a*	H_2N^-	+27.0	*a*
H_2O	−57.8	*a*	HO^-	−32.7	*a*
$H_2C{=}O$	−26.0	*a*			
CH_3NH_2	−5.5	*a*			
CH_3OH	−48.2	*a*	CH_3O^-	−33.2	*a*
			HS^-	−19.4	*a*
			NSO^-	<−33.9	*a*
CH_3OCH_3	−44	*a*			
CH_3COCH_3	−51.9	*a*	$CH_3COCH_2^-$	−45.2	*a*
CH_3COOH	−103.3	*a*	CH_3COO^-	−120.5	*a*
OCS	−34	*a*			
			$CH_2NO_2^-$	−27.2	*a*
CH_3SCH_3	−9.0	*a*	$CH_3SCH_2^-$	+18.4	*a*
SO_2	−70.9	*a*	SO_2^-	−96.3	*a*
			$C_5H_5^-$	+19.6	*a*
$CH_3CH_2SCH_3$	−14.2	*a*			
C_6H_6	+19.8	*a*	$C_6H_5^-$	+54.7	*a*
CS_2	+28	*a*			
$CH_3CH_2NO_2$	−24.4	*a*			
$C_6H_5CH_3$	+12.0	*a*			
c-$C_5H_5CH_3$	+25.1	*b*			
$CH_3OSO_2CH_3$	−115.5	*c*	$CH_3OSO_2^-$	−144	*d*

[a] Reference 10. [b] Calculated based on group additivity.[31] [c] Reference 32. [d] Based on the gas-phase acidity reported in the text and the appropriate neutral heat of formation.

Discussion

We can account for the observations reported herein with four general pathways by which an anion might react with dimethyl sulfite (Scheme I): (i) nucleophilic attack at sulfur, path a; (ii)

(30) Meot-Ner, M.; Kafafi, S. A. *J. Am. Chem. Soc.* **1988**, *110*, 6297–6303.
(31) Benson, S. W. *Thermochemical Kinetics*, 2nd ed.; Wiley & Sons: New York, 1976.
(32) Benson, S. W. *Chem. Rev.* **1978**, *78*, 23–35.

Scheme I. Generalized Reaction Scheme of the Gas-Phase Interactions of Anions with Dimethyl Sulfite

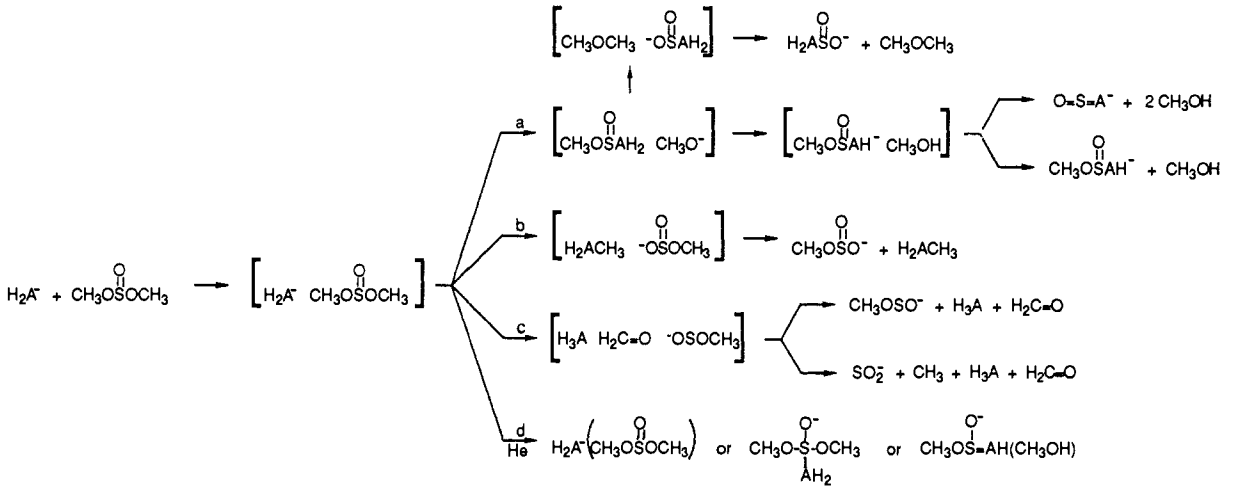

nucleophilic substitution at the methyl group, path b; (iii) elimination initiated by proton abstraction from the methyl group, path c; (iv) adduct/cluster formation, path d. Scheme I is not meant to be a complete mechanistic explanation and hence not all intermediates are shown. For example, the substitution process that takes place at sulfur may proceed via a tetravalent intermediate (not shown). The species within the square brackets are representations of some of the long-lived ion–dipole complexes that may exist along the reaction coordinate, not all of which are shown, and none of which are directly detected.

For all nucleophiles examined that displayed bimolecular reaction, the m/z 95 ion is formed as a significant product. Before considering the mechanism by which anions react with dimethyl sulfite, we discuss our data concerning the chemistry of the m/z 95 ion. We anticipated that $CH_3OSO_2^-$ would be a good leaving group for carbon-center substitution reactions based upon its expected relatively low basicity. The results of our attempts to experimentally bracket the proton affinity of $CH_3OSO_2^-$ are presented in Table II. Because we were unable to use CH_3OSO_2H as a neutral reagent, the only data available to us concerning the acidity of CH_3OSO_2H are derived from the reactions displayed by its conjugate base. Exclusive proton transfer is observed between trifluoracetic acid and the m/z 95 ion while no reaction is observed between either methanol or acetone and m/z 95. Such data roughly bracket the acidity of CH_3OSO_2H between 323 and 369 kcal mol^{-1}. Some proton transfer is observed from chloroacetic acid and acetyl acetone to m/z 95, though other pathways are also detected in these latter cases. For all acids examined that are less acidic than acetyl acetone ($\Delta H°_{acid}[CH_3COCH_2COCH_3]$ = 343 ± 2.4 kcal mol^{-1}), no proton transfer is directly observed. However, the upper limit on the bracketing experiments is somewhat obscured by the presence of the alternate chemical reaction shown in eq 5 for acetic acid, which is also detected for hydrogen sulfide, formic acid, acetyl acetone, and chloroacetic acid. Note that eq 5 can be considered to be a sulfur dioxide transfer process from methoxide ion to acetate ion.

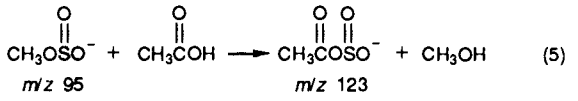

Consider the entire set of Brønsted acid–base reactions shown in Table II. Starting from CF_3CO_2H, as we decrease the acidity of the donor acid in small increments, we find that sole proton transfer gives way first to proton transfer with a minor amount of sulfur dioxide transfer. Further decrements in the neutral acidity reveals sulfur dioxide as the major process with only a minor amount of proton transfer. Even further decrements in the proton-donating ability of the acid results in sole SO_2 transfer until even that channel becomes too slow to observe. Unequivocally then, we can bracket the acidity of CH_3OSO_2H as being between 344 and 362 kcal mol^{-1}. However, on the basis of numerous

Scheme II[a]

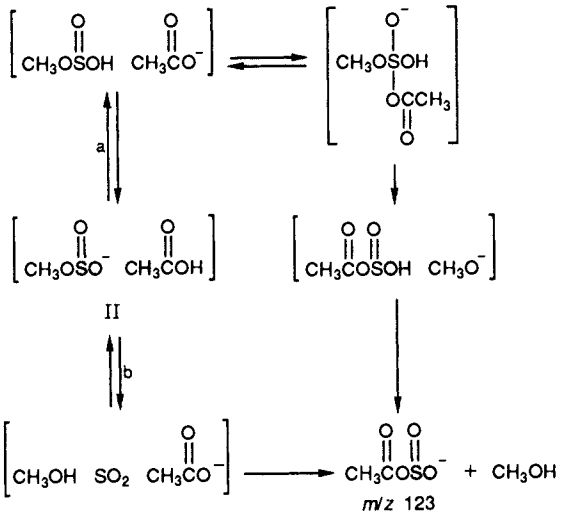

[a] Note that complex II is that initially formed from separated reactants, which are not shown.

observations that proton-transfer reactions are observed when exothermic, even in the presence of other, more exothermic channels, we interpret the data in Table II as follows. The changeover from all proton transfer to all sulfur dioxide transfer indicated in Table II is due to the proton-transfer reaction changing from exothermic to endothermic. With the proton transfer made slow by a thermochemical barrier, the sulfur dioxide transfer channel has a chance to dominate. On the basis of these data[10,33] we can assign a value of $\Delta H°_{acid}[CH_3OSO_2H]$ = 343 ± 4 kcal mol^{-1}. The facile sulfur dioxide transfer pathway that competes with proton transfer hinders a more precise bracketing of the proton affinity of m/z 95. The relatively low value for the proton affinity of $CH_3OSO_2^-$ is in accord with its facile displacement in a bimolecular substitution process by all of the nucleophiles examined in this work.

The sulfur dioxide transfer process shown in eq 5 is an intriguing transformation. As illustrated in Table II, sulfur dioxide transfer competes with direct proton transfer for neutral acids whose acidities are in the range of 336–344 kcal mol^{-1}. For acids less acidic than acetyl acetone, but at least as acidic as hydrogen sulfide, the SO_2 transfer pathway is a facile, quantitative process. Two mechanisms that account for this process are shown in Scheme II for acetic acid; both pathways originate from the ion–molecule encounter complex formed between acetic acid and $CH_3OSO_2^-$ (complex II).

(33) Bartmess, J. E.; McIver, R. T., Jr. In *Gas Phase Ion Chemistry*; Bowers, M. T., Ed.; Academic: New York, 1979; Vol. 2, Chapter 11.

The first pathway (a) in Scheme II involves an endothermic proton transfer (fueled by the ion–dipole complex energy) followed by formation of a tetravalent intermediate. Breakdown of the tetravalent intermediate in the contrathermodynamic direction followed by exothermic proton transfer gives rise to the observed products. We feel that this mechanism is unlikely because the tetravalent intermediate will prefer to extrude acetate rather than methoxide (i.e., return toward reactants). The alternate pathway (b) shown in Scheme II involves use of the ion–dipole complex energy to transfer methoxide from SO_2 to the proton in acetic acid with concomitant formation of acetate. Using the data in Table IV, we estimate that the energy needed for this process (neglecting ion solvation energies) as +7.7 kcal mol^{-1}. If acetone is used instead of acetic acid, we estimate that the energy needed for the first step of pathway b is +31.6 kcal mol^{-1}; this latter process is probably more endothermic than the available ion–solvation energy (typically 15–25 kcal mol^{-1}), which would account for the observed lack of reaction with acetone. We feel that the fragmentation of $CH_3OSO_2^-$ to CH_3O^- and SO_2 followed by proton transfer from acetic acid to methoxide is an unlikely route since the fragmentation step is endothermic by 39.9 kcal mol^{-1}, which is larger than the energy available within ion–molecule complex II.

With the four pathways of Scheme I in mind, consider the data from the amide reaction first. The major product observed at m/z 79, CH_3OSO^-, produced in 44% yield, can be envisioned as arising from elimination across a carbon–oxygen bond (Scheme I, path c; $H_2A^- = H_2N^-$). The m/z 64 ion, SO_2^-, can be formed by a minor fragmentation during the elimination of those CH_3OSO^- ions that obtain enough of the reaction exothermicity to surmount the fragmentation barrier.

Several observations support such a mechanistic assignment to the source of the m/z 64 ion. First, SO_2^- is only observed when CH_3OSO^- ion is observed. Second, SO_2^-, when formed, is only a fraction of the yield of CH_3OSO^-. Third, both CH_3OSO^- and SO_2^- are only detected for the strongest bases examined, and their combined yield drops off rapidly as the base strength is decreased. The combined yield of CH_3OSO^- and SO_2^- is 48% for amide (the strongest base examined), 10% for phenide (3.0 kcal mol^{-1} weaker a base than amide), 0.4% for the conjugate base of dimethyl sulfide (10.5 kcal mol^{-1} weaker than amide), and 20% for hydroxide (12.9 kcal mol^{-1} weaker a base than amide). Neither CH_3OSO^- nor SO_2^- was detected as a product ion from any other nucleophile examined and, in particular, for any nucleophilic base weaker than hydroxide. Fourth, the relative amount of SO_2^- as compared to the amount of CH_3OSO^- decreased as the reaction exothermicity of the elimination channel was decreased (by decreasing the proton affinity of the anionic base). Finally, there is no evidence that, in our flowing afterglow, CH_3OSO^- undergoes any further fragmentation due to the many thermal-energy collisions it undergoes with helium or due to its sampling from the flow tube into the quadrupole mass filter by the use of weak electric fields. Our suggested route for the formation of SO_2^-, by a unimolecular fragmentation of excited CH_3OSO^- ions produced in an elimination reaction, is similar in many ways to McDonald and Chowdhury's report of fragmentation of $CF_3CO_2^-$ (to CF_3^- + CO_2) produced in a highly exothermic S_N2 reaction.[34]

Also produced in 44% overall yield from the reaction of amide and dimethyl sulfite is $CH_3OSO_2^-$, m/z 95, which arises from bimolecular substitution at saturated carbon (path b in Scheme I). Nucleophilic substitution at methyl centers bearing leaving groups that are the conjugate bases of strong acids are well-known in the gas phase.[35] The two remaining minor products detected in the amide reaction are m/z 62 and 94. Both ions can be envisioned as arising from the same initial reaction in which amide adds to sulfur to form a tetravalent species, which may either be an intermediate or a transition state. For simplicity we will hereafter refer to it as an intermediate since such an assignment leads to clear interpretation and prediction. The tetravalent intermediate, once formed, breaks down by extruding methoxide, a much less basic anion than amide (Scheme I, path a). The methoxide so produced in the ion–dipole complex can abstract a proton from the newly formed nitrogen-containing neutral (followed by ion–dipole complex dissociation), giving rise to the m/z 94 ion, CH_3OSONH^-. Alternatively, if the methoxide so produced induces an elimination process by abstracting a proton from the nitrogen of the neutral within the complex, a ternary ion–molecule complex, [CH_3O^- OSNH $HOCH_3$], will be formed, which will then dissociate to give the weakest anionic base, NSO^- (m/z 62), and 2 equiv of methanol (note that no methoxide is observed to escape the complex). The m/z 62 ion, NSO^-, has previously been demonstrated to be formed in a fast reaction between amide and sulfur dioxide.[12] The mechanistic hypothesis for the reaction of amide at sulfur in dimethyl sulfite is illustrated in eq 6. The percentages shown above the arrows of the final step in eq 6 are taken from Table I and represent the absolute yields of the product channels depicted.

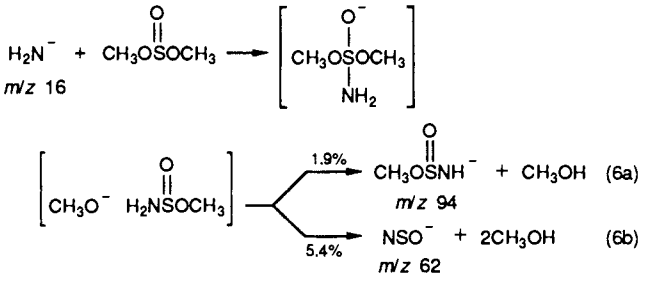

The reactions displayed when amide reacts with dimethyl sulfite are summarized in eq 7 (and in Table III according to reaction type), along with our estimates of the reaction exothermicities (where they are estimable), which are computed utilizing the data in Table IV. (In eq 7, "+10.0 kcal mol^{-1}" indicates a reaction channel that is exothermic by 10.0 kcal mol^{-1}.)

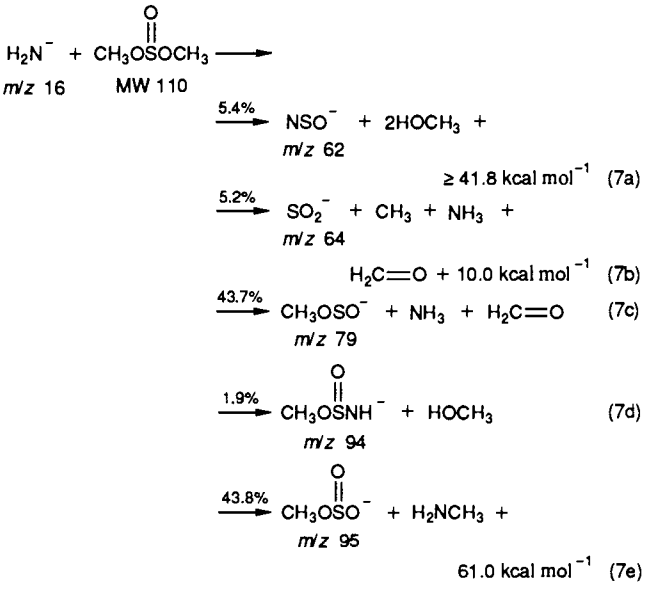

Thus 43.8% of the amide–dimethyl sulfite collisions lead to substitution at carbon, 48.9% to elimination across a C–O bond, and only 7.3% to substitution at the sulfur center. Since the observed efficiency is 1, *all* amide–dimethyl sulfite collisions lead to product formation; there are no nonproductive collisions. In addition to the primary reaction pathways displayed by amide ion with dimethyl sulfite, there is one secondary reaction in which the initial m/z 79 product ion reacts with a second molecule of dimethyl sulfite to yield additional amounts of m/z 95. This

(34) McDonald, R. N.; Chowdhury, A. K. *J. Am. Chem. Soc.* **1982**, *104*, 901–902.

(35) (a) Brauman, J. I.; Olmstead, W. N. *J. Am. Chem. Soc.* **1977**, *99*, 4219–4228. (b) Brauman, J. I.; Pellerite, M. J. *J. Am. Chem. Soc.* **1980**, *102*, 5993–5999. (c) Riveros, J. M.; Jose, S. M.; Takashima, K. In *Advances in Physical Organic Chemistry*; Gold, V., Bethell, D., Eds.; Academic Press: New York, 1985; Vol. 21, pp 197–240. (d) Brauman, J. I.; Dodd, J. A.; Han, C.-C. In *Nucleophilicity*; Harris, J. M., McManus, S. P., Eds.; Advances in Chemistry Series 215; American Chemical Society: Washington, DC, 1987; Chapter 2.

observation is interpreted as an additional substitution process (eq 8) and is observed for every system in which the original nucleophile produces CH_3OSO^-. The exact structure of the neutral product of the substitution process shown in eq 8 is unclear.

$$\underset{m/z\ 79}{CH_3OSO^-} + \underset{\text{MW } 110}{CH_3O\overset{\overset{O}{\|}}{S}OCH_3} \rightarrow \underset{m/z\ 95}{CH_3O\overset{\overset{O}{\|}}{S}O^-} + [CH_3OSOCH_3] \quad (8)$$

Hydroxide, a nucleophile 12.9 kcal mol^{-1} weaker a base than amide, gives three products from reaction with dimethyl sulfite, including 19.5% elimination products (Tables I and III, both CH_3OSO^- and SO_2^- are observed). The major product ion from the hydroxide reaction is $CH_3OSO_2^-$ Unfortunately, we cannot determine, without utilization of oxygen-18 labeled hydroxide ion, whether any or all of the m/z 95 product ion arises from reaction at sulfur. On the basis of all the data reported herein, it is highly likely that the m/z 95 ion is produced by reaction *both* at sulfur and at carbon. The two-methanol loss channel via reaction at sulfur shown in Scheme I, path a, is precluded for the hydroxide reaction since the incoming nucleophile only has a single proton. The hydroxide–dimethyl sulfite reactions are summarized in eq 9, which can be compared to the amide reaction (eq 7). The largest difference between the reactions displayed by H_2N^- and HO^- is the amount of elimination versus substitution that occurs; considerably more elimination occurs for the stronger of the two bases in these two fast reactions.

$$\underset{m/z\ 17}{HO^-} + \underset{\text{MW } 110}{CH_3O\overset{\overset{O}{\|}}{S}OCH_3} \longrightarrow$$

$$\xrightarrow{1.2\%} \underset{m/z\ 64}{SO_2^-} + CH_3 + H_2O + H_2C{=}O - 2.9 \text{ kcal mol}^{-1} \quad (9a)$$

$$\xrightarrow{18.3\%} \underset{m/z\ 79}{CH_3OSO^-} + H_2O + H_2C{=}O \quad (9b)$$

$$\xrightarrow{80.5\%} \underset{m/z\ 95}{CH_3O\overset{\overset{O}{\|}}{S}O^-} + HOCH_3 + 44.0 \text{ kcal mol}^{-1} \quad (9c)$$

Methoxide reacts efficiently with dimethyl sulfite and gives $CH_3OSO_2^-$ as the only ion product (the displacement reaction is exothermic by 39 kcal mol^{-1}); evidently methoxide is not sufficiently strong enough as a base to induce the elimination reaction (i.e., Scheme I, pathway c). Using the values in Table IV, we estimate that ΔH_{rxn} for the elimination and subsequent fragmentation pathway is +13 kcal mol^{-1} (i.e., the hypothetical methoxide reaction that is related to eq 9a). Labeling the methoxide (e.g., CD_3O^-) allows us to observe incorporation of the original nucleophile into the reaction product (eq 10).

$$\underset{m/z\ 34}{CD_3O^-} + \underset{\text{MW } 110}{CH_3O\overset{\overset{O}{\|}}{S}OCH_3} \xrightarrow{83.2\%} \underset{m/z\ 95}{CH_3O\overset{\overset{O}{\|}}{S}O^-} + CD_3OCH_3 \quad (10a)$$

$$\xrightarrow{16.8\%} \underset{m/z\ 98}{CD_3O\overset{\overset{O}{\|}}{S}O^-} + CH_3OCH_3 \quad (10b)$$

The product distribution for the reaction of CD_3O^- with dimethyl sulfite reveals the existence of two competitive pathways, substitution at carbon and at sulfur, but it does not *directly* reveal the competitive rates for these two channels. In order to unravel the relative rate coefficients for attack at carbon (k_{nuc}) versus that for attack at sulfur (k_{tet}), one must consider the model shown in Scheme III. In our model, when CD_3O^- encounters dimethyl sulfite under the thermally equilibrated conditions of the FA, an ion–dipole complex (the first ion–neutral pair enclosed by brackets in Scheme III) between those two distinct species is formed. This first-formed complex has two competitive reaction channels open to it, either irreversible nucleophilic substitution at carbon (dimethyl ether does not undergo displacement at carbon with anions in the gas phase[36]) or reaction at sulfur to form a tetravalent intermediate. This tetravalent intermediate, which is never observed in our experiment, is considered to have three equivalent methoxide groups. The tetravalent intermediate always breaks down by extrusion of a methoxide group; the ratio of CD_3O^- to CH_3O^- loss is simply dictated by statistics (at this point, we are neglecting any isotope effects, consideration of which should favor CH_3O^- loss over CD_3O^- since the deuterated methoxide is a 0.5 kcal mol^{-1} stronger base than the protio methoxide).[26] If CD_3O^- is extruded, the initially formed complex is regenerated and faces the same branching as it did before. If CH_3O^- is extruded from the tetravalent adduct, a unique ion–dipole complex is formed between methoxide-h_3 and d_3-labeled dimethyl sulfite (the last ion–neutral pair enclosed by brackets in Scheme III). This latter complex has the same options open to it that the first-formed complex had (irreversible substitution at carbon and addition to sulfur to re-form the tetravalent adduct). Thus to properly define the relative ease of reaction at carbon versus sulfur, one needs to extract the relative rate coefficients, k_{tet} and k_{nuc}.

A simple computer algorithm, which starts with the assumption that m/z 95 and 98 both arise from a long-lived complex of the type shown in Scheme III, calculates the amount of $CH_3OSO_2^-$ and $CD_3OSO_2^-$ formed as the ratio of k_{tet} to k_{nuc} is varied. Comparing the experimentally observed amounts of the two products to those calculated for various rate ratios leads to the conclusion that k_{tet}/k_{nuc} is 1.016 or that when methoxide encounters dimethyl sulfite, it is equally likely to react at the carbon or the sulfur sites. As an illustration of the response of the ratio of k_{tet} to k_{nuc} to calculated product distributions, increasing or decreasing the best fit ratio by 10% predicts 82.4% and 84.1% m/z 95, respectively, which can be considered to be our error limits. We have omitted a dissociation channel for the two ion–dipole complexes in Scheme III (i.e., dissociation to form methoxide ion), because the overall reaction is fast ($k_{obs} = 2.2 \times 10^{-9}$) and occurs on nearly every collision, and CH_3O^- is not directly observed. Since addition to sulfur is a "dead-end" reaction, all the reaction products are eventually trapped in the displacement channel. Thus the observation of 16.8% $CD_3OSO_2^-$ from the reaction of CD_3O^- with dimethyl sulfite indicates equal intrinsic reactivities of carbon and sulfur. While we have not proven that the tetravalent adduct is a true intermediate on this reaction coordinate, prior experimental[5c,37] and theoretical[3,38] studies indicate that it is likely to be such. However, it is important to note that our interpretation of the nealy equal reactivities toward the two sites will not substantially change if the tetravalent species is a transition state rather than an intermediate.

HS^- reacts slowly but completely with dimethyl sulfite and gives principally substitution products (the only other product is 1.7% of the adduct ion at 0.30 Torr of helium). Several anions, which are stronger bases than HS^-, are observed to be slower reacting and/or to give adduct only (vide infra) in accord with the well-known[39] trend from the condensed phase that sulfur nucleophiles are better than oxygen nucleophiles despite the opposite basicity order. We interpret the lack of products from reaction at the sulfur site in dimethyl sulfite as follows: when any tetravalent adduct that is formed breaks down, it prefers to extrude HS^- (the weaker base) over CH_3O^-. For this reason, we are unable to compare

(36) (a) DePuy, C. H.; Bierbaum, V. M. *J. Am. Chem. Soc.* **1981**, *103*, 5034–5038. (b) Grabowski, J. J.; DePuy, C. H.; Bierbaum, V. M. *J. Am. Chem. Soc.* **1983**, *105*, 2565–2571.

(37) (a) Bowie, J. H.; Williams, B. D. *Aust. J. Chem.* **1974**, *27*, 1923–1927. (b) Bohme, D. K.; Mackay, G. I.; Tanner, S. D. *J. Am. Chem. Soc.* **1980**, *102*, 407–409.

(38) (a) Weiner, S. J.; Singh, U. C.; Kollman, P. A. *J. Am. Chem. Soc.* **1985**, *107*, 2219–2229. (b) Madura, J. D.; Jorgensen, W. L. *J. Am. Chem. Soc.* **1986**, *108*, 2517–2527. (c) Cardy, H.; Loudet, M.; Poulicard, J.; Ollivier, J.; Poquet, E. *Chem. Phys.* **1989**, *131*, 227–243.

(39) (a) March, J. *Advanced Organic Chemistry*, 3rd ed.; Wiley & Sons: New York, 1985; pp 304–310. (b) Lowry, T. H.; Richardson, K. S. *Mechanism and Theory in Organic Chemistry*, 3rd ed.; Harper and Row: New York, 1987; pp 367–373.

Scheme III. Kinetic Model Used To Determine the Efficacy of Methoxide Reacting at Sulfur and Carbon Sites in Dimethyl Sulfite

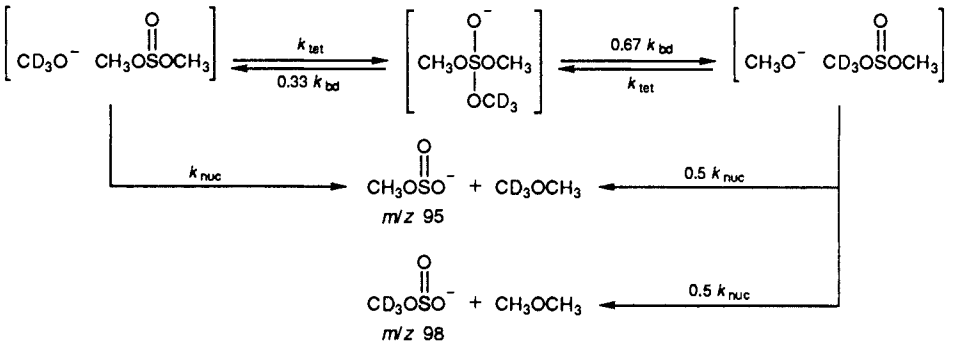

rates of reaction at carbon to sulfur within the initial ion–neutral complex since any addition to sulfur is immediately undone and the only observed reaction product results from substitution at carbon. From amide to methoxide, there is a large decrease in base strength and a large increase in the amount of sulfur reaction path for dimethyl sulfite. Since HS^- is a much weaker base than methoxide, we might expect HS^- to add to sulfur more easily than to instigate a displacement reaction at carbon. Such a first-order expectation will be modified by the energies (basicities of the ions) of the HS^-–$CH_3OSO_2CH_3$ ion–dipole complex as compared to the tetravalent adduct, a consideration that we are not fully able to evaluate.

Allyl anion reacts with dimethyl sulfite by substitution both at carbon (43.6%) and at sulfur (56.4%); no elimination is observed at all for the allyl anion. The interpretation of the observations for the allyl anion reacting with dimethyl sulfite are summarized in eq 11. As we observed in the amide ion reaction, the two-methanol loss pathway for the sulfur site reaction is favored over the one-methanol loss pathway (i.e., compare eq 11a and 11c).

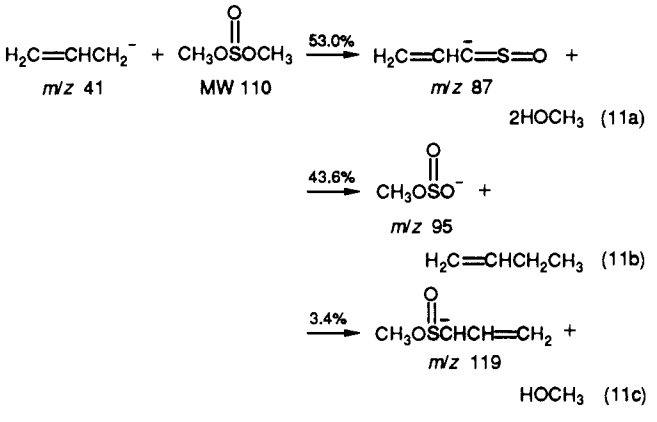

Benzyl anion (eq 12) shows the same product channels as allyl anion. Contrasting benzyl and allyl anion reactions, we see that allyl anion, the stronger base, is about twice as efficient as benzyl anion (efficiencies of 50% and 28% respectively) and that the weaker base gives more sulfur substitution products (87.7%) as compared to allyl anion (56.4%). We interpret these data to

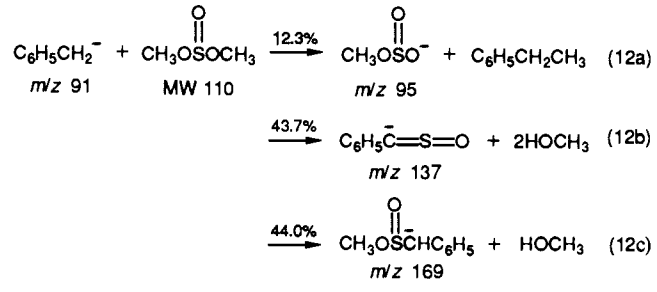

indicate that the carbon substitution path is more sensitive to reaction exothermicity than sulfur substitution, and the main difference between allyl and benzyl anion is simply due to a decrease in the rate coefficient for carbon substitution with a smaller decrease in the rate coefficient for reaction at sulfur Again in comparison of allyl to benzyl anions, the two-methanol loss as compared to the one-methanol loss channel is much more important for allyl (ratio of eq 11a to 11c is 15.6) than benzyl (ratio is 0.99). Because methoxide and benzyl anion have identical proton affinities and therefore, by that measure, have comparable leaving group abilities, it is possible that the intrinsic rate for addition to sulfur versus reaction at carbon is considerably higher than that reflected directly in the product distribution in a manner analogous to that discussed above for methoxide. Hence we must consider the ratio of S to C rates obtained *directly* from observed product distributions to be a lower limit to the intrinsic reactivity of those two sites with benzyl anion.

The observations for pentadienyl anion reacting with dimethyl sulfite are summarized in eq 13. First, consider the ratio of

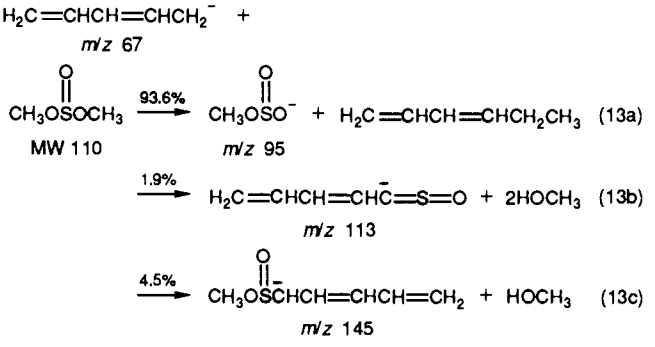

two-methanol loss to one-methanol loss channels for pentadienyl anion. This value (0.42) is lower than that for either allyl or benzyl, which is in accord with our mechanistic interpretations so far presented. As the hydrocarbon base is made less basic, the sulfur substitution reaction becomes less exothermic resulting in less fragmentation into the two-methanol loss channel. Also, pentadienyl anion shows mostly products from reaction at carbon and at a much lower reaction efficiency (Eff = 0.23%) than either benzyl or allyl anions. We suggest that this is a manifestation of the best leaving group (i.e., the weakest base) being extruded from the tetravalent sulfur adduct. For allyl and benzyl anions, the best leaving group in the tetravalent adduct is methoxide, while for pentadienyl anion, it is the reactant ion. As a result, only rarely does the tetravalent adduct in the pentadienyl reaction break down by extrusion of methoxide, the products of which are immediately trapped by the favorable proton transfer. The low reaction efficiency is a reflection of the inefficiency of the substitution process at carbon and the proclivity of the tetravalent adduct to return to reactants. The qualitative observations for cyclohexadienide confirm these mechanistic interpretations. Cyclohexadienyl anion gives more substitution at carbon than at sulfur and is intermediate in basicity to pentadienyl and benzyl anions. Cyclopentadienyl anion, the weakest hydrocarbon base we examined, is so weakly nucleophilic that no substitution is observed (even though it is exothermic by 23 kcal mol^{-1}); rather, slow adduct formation is the only reaction detected. If addition to sulfur is occurring, then for cyclopentadienyl anion and dimethyl sulfite, the tetravalent

adduct never breaks down by extruding the much more strongly basic methoxide ion, as distinctive products from this channel are not detected.

Of the five delocalized, anionic, hydrocarbon bases just mentioned, allyl ion, since it is the best thermodynamic base of the lot, is the one that might be expected to give elimination products. In fact, allyl ion does not produce any elimination products, while hydroxide, a localized base of identical thermodynamic basicity to allyl ion, yields 19.5% elimination product. These results are in accord with our earlier observations of how anions react with dimethyl disulfide, in which allyl anion was also found to be poor as a base for an elimination reaction, in stark contrast to HO^-.[4] Allyl ion is a good nucleophile toward sulfur centers, both in dimethyl sulfite and in dimethyl disulfide. The observation of significant amounts of S_N2 reaction between allyl ion and dimethyl sulfite is in accord with the rapid rates of substitution noted between allyl anion and methyl bromide or methyl chloride.[34] Thus allyl anion kinetically appears to be a much better nucleophile than a base, especially compared to HO^-, and, when given a choice, will instigate substitution processes with a substrate rather than elimination processes.

We examined four delocalized anions in which the negative charge is spread over both carbon and heteroatom sites: cyanomethide, anilide, acetaldehyde enolate, and nitromethide. Cyanomethide is more basic than pentadienyl anion and less basic than cyclohexadienide, so we might reasonably expect to see some (i.e., more than 6%, less than ~40%) products from reaction at sulfur. Instead, moderately fast reaction produces only carbon substitution (eq 14). Anilide displays the same behavior as

$$\underset{m/z\ 40}{NCCH_2^-} + \underset{\text{MW } 110}{CH_3OSOCH_3} \xrightarrow{100\%} \underset{m/z\ 95}{CH_3OSO^-} + C_3H_5N \qquad (14)$$

cyanomethide except the reaction is considerably slower. Acetaldehyde enolate gives a moderately fast reaction (efficiency of 4.6%) and forms principally the m/z 95 carbon substitution product in addition to a significant amount of the adduct. Nitromethide gives only slow formation of the adduct. On initial inspection, anilide, acetaldehyde enolate, and nitromethide follow the general mechanistic interpretation being developed; all three are weak bases compared to methoxide and hence any tetravalent intermediate formed from dimethyl sulfite will break down to re-form reactants, precluding sulfur substitution products from being formed. Nitromethide is even too poor a nucleophile to give rise to the exothermic carbon substitution product ($\Delta H_{rxn} = -25.7$ kcal mol^{-1}). Close inspection reveals that the rates of acetaldehyde enolate and cyanomethide (both "too" fast), and the product distribution from cyanomethide (no sulfur substitution) reactions are not in accord with the trend so far developed. We think that these data suggest that both cyanomethide and acetaldehyde enolate are reacting with dimethyl sulfite, not via their carbon center but rather through their heteroatom center. This latter explanation nicely accounts for the data for cyanomethide, anilide, and acetaldehyde enolate ions compared to that for cyclohexadienide and pentadienide. Such an interpretation implies that heteroatom sites in ambident nucleophiles display an enhanced reactivity for carbon vs sulfur sites in dimethyl sulfite compared to hydrocarbon anions of similar basicity. Cyclohexanone enolate in the gas phase has been demonstrated to be a good nucleophile toward sp^3 C (CH_3I) yielding as the exclusive reaction product O-alkylation.[40] Furthermore, Brickhouse and Squires have recently presented strong arguments that aldehyde enolates react with 6,6-dimethylfulvene to a large extent, by way of the oxygen center, in accord with our observations here.[41] Further investigations and considerations of these ideas are needed.

The three final nucleophiles to consider are the conjugate bases of benzene, dimethyl sulfide, and furan, all of which *might* be considered to be localized carbanions. The conjugate base of benzene displays a rapid reaction with dimethyl sulfite giving the bimolecular substitution product at carbon as the major process (78.3%) and 10% elimination products. The remainder of the reaction products, 11.7%, are conceived of as arising from initial nucleophilic reaction at sulfur, followed by extrusion of the best leaving group, methoxide. However, before methoxide departs the complex (it is not detected as a product ion) it reacts with the neutral component of the ion–dipole complex, not by a proton transfer since there are no acidic protons but by a displacement process, giving rise to the phenyl sulfinate anion (m/z 141; top variant of path a in Scheme I). This bimolecular substitution process, occurring in an ion–dipole complex formed as the result of an ion–molecule reaction is a demonstration of the rare occurrence of an S_N2 following a previous reaction, both of which occur consecutively in the same encounter complex.[42] All phenide anion/dimethyl sulfite pathways are summarized in eq 15.

$$\underset{m/z\ 77}{C_6H_5^-} + \underset{\text{MW } 110}{CH_3OSOCH_3} \xrightarrow{0.5\%} \underset{m/z\ 95}{SO_2^-} + C_6H_6 + H_2C{=}O + \quad 6.9 \text{ kcal mol}^{-1} \qquad (15a)$$

$$\xrightarrow{9.5\%} \underset{m/z\ 79}{CH_3OSO^-} + C_6H_6 + H_2C{=}O \qquad (15b)$$

$$\xrightarrow{78.3\%} \underset{m/z\ 95}{CH_3OSO^-} + C_6H_5CH_3 + \quad 71.2 \text{ kcal mol}^{-1} \qquad (15c)$$

$$\xrightarrow{11.7\%} \underset{m/z\ 141}{C_6H_5OSO^-} + CH_3OCH_3 \qquad (15d)$$

The major channel for the nucleophile $CH_3SCH_2^-$ with dimethyl sulfite (eq 16) is S_N2 displacement at carbon, the same as was observed for phenide. (Note that, from the data in Table IV, reaction 16a is estimated to be 0.6 kcal mol^{-1} endothermic and reaction 16c to be 61.1 kcal mol^{-1} exothermic.)

$$\underset{m/z\ 61}{CH_3SCH_2^-} + \underset{\text{MW } 110}{CH_3OSOCH_3} \xrightarrow{\text{trace}} \underset{m/z\ 64}{SO_2^-} + CH_3 + \quad CH_3SCH_3 + H_2C{=}O \qquad (16a)$$

$$\xrightarrow{0.4\%} \underset{m/z\ 79}{CH_3OSO^-} + \quad CH_3SCH_3 + H_2C{=}O \qquad (16b)$$

$$\xrightarrow{61.2\%} \underset{m/z\ 95}{CH_3OSO^-} + CH_3SCH_2CH_3 \qquad (16c)$$

$$\xrightarrow{33.1\%} \underset{m/z\ 107}{CH_3SC{=}S{=}O} + 2HOCH_3 \qquad (16d)$$

$$\xrightarrow{5.3\%} \underset{m/z\ 139}{CH_3OSCHSCH_3} + HOCH_3 \qquad (16e)$$

Only 0.4% of all product-producing ion–neutral collisions between $CH_3SCH_2^-$ and $CH_3OSO_2CH_3$ lead to elimination products, while 38.4% of the successful collisions lead to products resulting from reaction at sulfur. Contrast the dimethyl ether forming pathway for phenide ion and the conjugate base of dimethyl sulfide: formation of the methoxide-containing ion–dipole complex on path a (Scheme I) preferentially results in subsequent pro-

(40) Jones, M. E.; Kass, S. R.; Filley, J.; Barkley, R. M.; Ellison, G. B. *J. Am. Chem. Soc.* **1985**, *107*, 109–115.

(41) Brickhouse, M. D.; Squires, R. R. *J. Am. Chem. Soc.* **1988**, *110*, 2706–2714.

(42) An analogous observation has been reported for CD_3O^- with trimethyl phosphite: Anderson, D. R.; DePuy, C. H.; Filley, J.; Bierbaum, V. M. *J. Am. Chem. Soc.* **1984**, *106*, 6513–6517.

ton-transfer processes, rather than substitution at carbon since no $CH_3SCH_2SO_2^-$ is detected in the $CH_3SCH_2^-$ and $CH_3OSO_2CH_3$ system, but $C_6H_5SO_2^-$ is readily observed when phenide is the nucleophile.

The conjugate base of furan, which is less basic[25] than hydroxide, shows approximately equal amounts of substitution at carbon and sulfur (eq 17). The reaction at sulfur yields products

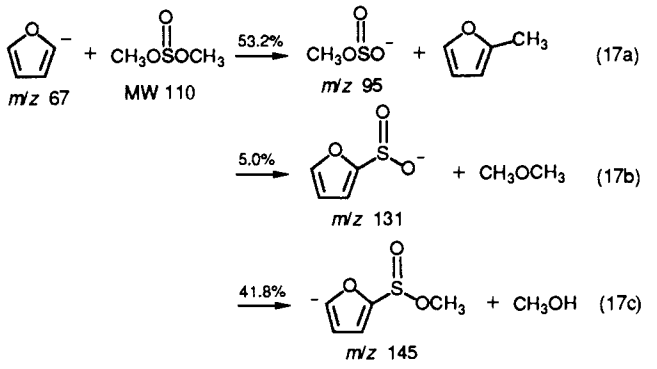

resulting from proton transfer (i.e., the m/z 145 product ion) as well as displacement at methyl (yielding the m/z 131 product ion), though as we noted earlier, those products from proton transfer are greatly preferred. It is not clear which proton is being lost in the abstraction process (eq 17c), but inductive arguments suggest that it is the proton α to the oxygen in the furan ring. These results confirm for the first time, that even for an ion–neutral pair generated by an ion–molecule reaction, proton transfer (e.g., eq 17c) is kinetically more feasible than a much more exothermic substitution at carbon (e.g., eq 17b). In addition to the primary reaction pathways displayed, there is one secondary reaction in which the m/z 145 ion attacks the carbon in another molecule of dimethyl sulfite to yield additional amounts of the m/z 95 ion.

Consider the product distributions observed for these latter three strongly basic, localized carbanions (eq 15–17 and Table III). As compared to the strong, localized bases amide and hydroxide, the localized carbon bases yield much smaller amounts of elimination product (e.g., 0.4% from $CH_3SCH_2^-$ versus 19.5% from the 2.4 kcal mol^{-1} *less* basic HO^-). We interpret this to mean that localized carbon bases are kinetically slower at instigating elimination reactions than are heteroatomic bases of similar base strength. Thus we see that localized carbon bases are better than delocalized carbon bases for elimination reactions but not nearly as good as localized heteroatomic bases. The localized carbon bases are much better nucleophiles toward carbon than a delocalized base of similar proton affinity; these differences are distinct despite both reactions being equally efficient.

Conclusion

A variety of anions were observed to react with dimethyl sulfite. Four reaction pathways account for the primary reaction products: (i) nucleophilic attack at sulfur; (ii) nucleophilic substitution at the methyl group; (iii) elimination initiated by proton abstraction from the methyl group;[43] (iv) adduct–cluster formation. The primary factor in determining which of these four pathways occurs is the structure of the anion while the proton affinity of the nucleophile is an important but secondary consideration. Anions with similar proton affinities, but different structures, give different product distributions, but with equally fast reactions. Strong, localized heteroatomic bases such as amide and hydroxide yield larger amounts of elimination products as compared to localized carbon bases of similar proton affinity, e.g., phenide and the conjugate base of dimethyl sulfide. No elimination products were observed for anions less basic than hydroxide, a manifestation that this pathway is controlled by *kinetic* basicity. Localized heteroatomic and carbon bases are more nucleophilic at carbon than are delocalized carbon bases. For nucleophilic attack at sulfur the opposite trend is found, delocalized carbon bases being most nucleophilic at this site. The high degree of selectivity is independent of the efficiency of the overall reaction. These data provide guidelines concerning anion choice for designing gas-phase ion studies that would emphasize $B_{AC}2$ type reactions over S_N2 or E2 (or any other selection). For example to study reactions at a carbonyl site while remaining relatively free of other reaction channels, one should use delocalized carbanion bases. As another example, to consider sp^3 C versus sp^2 C reactivity in a common molecule, choose a localized carbanion such as the conjugate base of dimethyl sulfide or furan. As exemplified by the CH_3O^- and $CH_3OSO_2CH_3$ data, the relative reactivity for two different sites in a common molecule is extractable from the observed product distribution by application of an appropriate mechanistic model. From the combination of the studies on dimethyl disulfide[4] and dimethyl carbonate[44] with the net studies reported here on dimethyl sulfite, a clear picture is emerging about predicting how any anion will select among competitive reaction channels for a given neutral.

Acknowledgment. We gratefully acknowledge financial support of this work by a National Science Foundation Presidential Young Investigator Award (Grant CHE-8552742). We also thank Dr. Yongchun Tang for valuable assistance in carrying out a few of the experiments reported here.

(43) In many ways, this process is analogous to that in the Swern oxidation: Omura, K.; Swern, D. *Tetrahedron* **1978**, *34*, 1651–1660.

(44) Grabowski, J. J.; Roy, P. D. Unpublished results.